Contents

I Introduction

If you look at the radiation of a radioactive source, you'll find an isotropic distribution. That means it has no preferred direction. This behavior is explained by the statistically isotropic distribution of the nuclear spin, because the emitted γ-quantum is related to the nuclear spin.
If a nucleus is in an excited state, which decays into an other excited state before decaying into the ground state, you can choose the direction of the first γ-Quantum as a quantification axis and observe the direction of the following γ-Quantum emitted by second decay. With a changing nuclear spin during the decay, you get degenerated sub-states given by the magnetic quantum number m. The choosing of a quantification axis annihilates the uniform distribution of the m-states and therefore annihilates the isotropic distribution of the radiation field emitted by the second decay (referring to the quantification axis).
With the conservation of angular momentum it is reasonable to assume, that the change of the nuclear spin during a decay is caused by the emitted radiation and the angular momentum it is carrying. The radiation carrying an angular momentum is called "multipole radiation". The properties of the multipole radiation are based on the angular momentum and the parity of the radiation.
In this experiment we measure the angular distribution of a γ-γ-cascade. This distribution gives us information about the multipole radiation and therefore we can determine the nuclear spins of the involved states.

II Theoretical foundation

2.1 Basics

First of all we want to sum up the basics for the understanding of the physical foundation before we discuss the actual physics, that happen at the experiment.

2.1.1 Nuclear spin

Analog to the electron, the proton and neutron also have a intrinsic angular momentum (spin) of $\frac{1}{2} \cdot \hbar$. Usually spins are expressed in the unit $\hbar$. That's why they're called $\frac{1}{2}$-particles or fermions. For a system consisting of many fermions, the total intrinsic angular momentum is the vector sum of each intrinsic angular momentum component. So nuclei with an even number of components have a whole-number spin $(0, 1, 2, ...)$ and nuclei with an odd number of components have a half-number spin $(\frac{1}{2}, \frac{3}{2}, ...)$.
The orbital angular momentum is behaving in the same way as the intrinsic angular momentum and by adding both together we get the total angular momentum, which is called the nuclear spin.

2.1.2 Quantum numbers for single particles

In quantum mechanics the state of a particle is fully described by its wave function, which is a solution of the wave equation of the system. The function depends on several parameters which are called the "quantum numbers". Similar to atom physics, the state of a nucleus can be described by its quantum numbers. Mostly the following quantum numbers are used to describe the state of a nucleus:

Orbital Quantum Number l
This quantum number gives the value of the orbital angular momentum with the absolute value $\hbar \cdot \sqrt{l(l+1)}$ and can have the values $0, 1, 2, ...$. Using the nomenclature of the atomic spectroscopy, the states are called:

$l = 0$ *s-state (sharp)*
$l = 1$ *p-state (principal)*
$l = 2$ *d-state (diffuse)*
$l = 3$ *f-state (fundamental)*
$l = 4$ *g-state*
$l = 5$ *h-state*
.
.
.

and the following go on alphabetically.

Magnetic Orbital Quantum Number m_l
This value gives the component of l in a characteristic direction, for example along an external magnetic field. It has $(2l + 1)$ whole numbered values $-l, -l + 1, ..., 0, ..., l - 1, l$.

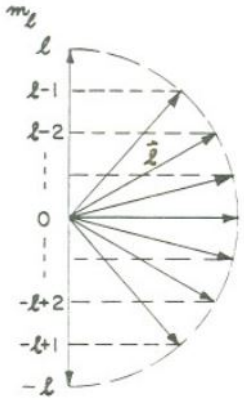

Figure 1: Projection of m_l, Source [8]

Spin Quantum Number s
The intrinsic angular momentum is called SPIN. Its absolute value is $\hbar \cdot \sqrt{s(s+1)}$ and has for bosons a whole numbered value and for fermions a half numbered value.

Magnetic Spin Quantum Number m_s
This value gives the component of s in a characteristic direction, for example along an external magnetic field. For $s = 0$ is $m_s = 0$ and for $s = \frac{1}{2}$ is $m_s = \pm\frac{1}{2}$, because after the vector model the spin can only be orientated parallel or anti-parallel to the characteristic direction.

Quantum Number Of The Total Angular Moment j
The total angular moment is characterized by the vector sum of the spin and the orbital angular momentum:

$$\vec{j} = \vec{s} + \vec{l} \tag{1}$$

The absolute value is $\hbar \cdot \sqrt{j(j+1)}$

Magnetic Quantum Number Of The Total Angular Moment m_j
This value gives the component of j in a characteristic direction, for example along an external magnetic field. Mostly it's just called m instead of m_j. It can have positive or negative values with a step of one. And analog to the other magnetic quantum numbers it has $(2j + 1)$ different values.

2.1.3 Angular moment of the nucleus

Every quantum state of the nucleus is built by a number of particles whose orbital angular momenta and spins are summed up and result in the total angular moment. The angular momentum of a state is characterized by the quantum number I (or sometimes J) with the absolute value $\hbar \cdot \sqrt{I(I+1)}$. The value of I is determined by the direct sum over all j_i:

$$\vec{I} = \sum_i \vec{j_i} \tag{2}$$

or the vector sum of the orbital angular momenta and spins:

$$\vec{I} = \vec{L} + \vec{S}, \tag{3}$$

with $\vec{L} = \sum_i \vec{l_i}$ and $\vec{S}p = \sum_i \vec{s_i}$.

2.1.4 Parity

With the probability density given by the square of the wave function, it is impossible to measure physically if the wave function is symmetric or anti-symmetric by inverting the space coordinates.

$$\psi(\vec{r}) = \psi(-\vec{r}) \tag{4}$$
$$\psi(\vec{r}) = -\psi(-\vec{r}) \tag{5}$$

If the parity is symmetric it's called *even* (or +) and if it's anti-symmetric its called *odd* (or -). To give the parity a physical meaning it's necessary to explain the correlation of the orbital angular momentum and the parity.

The wave function $\psi(r, \vartheta, \varphi)$ of a single (non-relativistic) nucleus in a state with orbital angular momentum l transforms in polar coordinate mirroring as the following

$$r \to r$$
$$\vartheta \to \pi - \vartheta$$
$$\varphi \to \pi + \varphi$$

The wave function can be written as

$$\psi(r, \vartheta, \varphi) = f(r) \cdot Y_{lm}(\vartheta, \varphi) \tag{6}$$

with the spherical harmonics

$$Y_{lm}(\vartheta, \varphi) = P_l^m(cos(\vartheta)) \cdot e^{i \cdot m \cdot \varphi} \tag{7}$$

which are depending on the quantum magnetic number m and the orbital angular momentum l. $P_l^m(cos(\vartheta))$ are the Legendre-Polynomials.

If we replace $\varphi \to \pi + \varphi$ we have to multiply $e^{i \cdot m \cdot \varphi}$ with $(-1)^m$ and by replacing $\vartheta \to \pi - \vartheta$ we get $P_l^m(-cos(\vartheta)) = (-1)^{l-m} \cdot P_l^m(-cos(\vartheta))$ what means we have to multiply the whole spherical harmonic $Y_{lm}(\vartheta, \varphi)$ with $(-1)^l$.
So a state with even l has an even parity and a state with odd l has an odd parity.

2.2 Electromagnetic Transitions

2.2.1 Shell Model

The energy distribution of the nucleons in the nucleus is given by the potential in the nucleus. The boundary condition lead to a discrete distribution of allowed states. Because the nucleons are fermions the have to obey the Pauli exclusion principle, which says, that same particles have to differ in their properties. These properties are described by the quantum numbers (see [2.1]). This leads to a shell model similar to the shell model of the atom shell, where the states (with their different quantum numbers) are filled in regard of their energy. But the potential inside the nucleus is much more complex than in the atom shell, because of the strong interaction between the nucleons. A good way to describe it is the Wood-Saxon-Potential.

$$V(x) = -\frac{V_0}{1 + \exp\left(\frac{r - R_0}{b_0}\right)}$$

It's a compromise of a box potential and the potential of the harmonic oscillator.

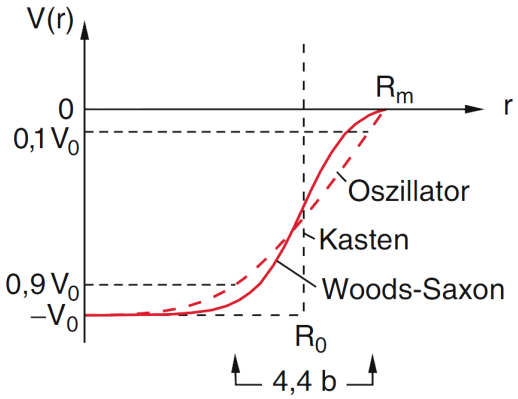

Figure 2: Wood-Saxon-Potential. Source: [3]

This potential gives us the following shell model for neutrons and protons. Where the potential of the protons is shifted towards the potential of the neutrons, because of their charge and their slightly different mass.

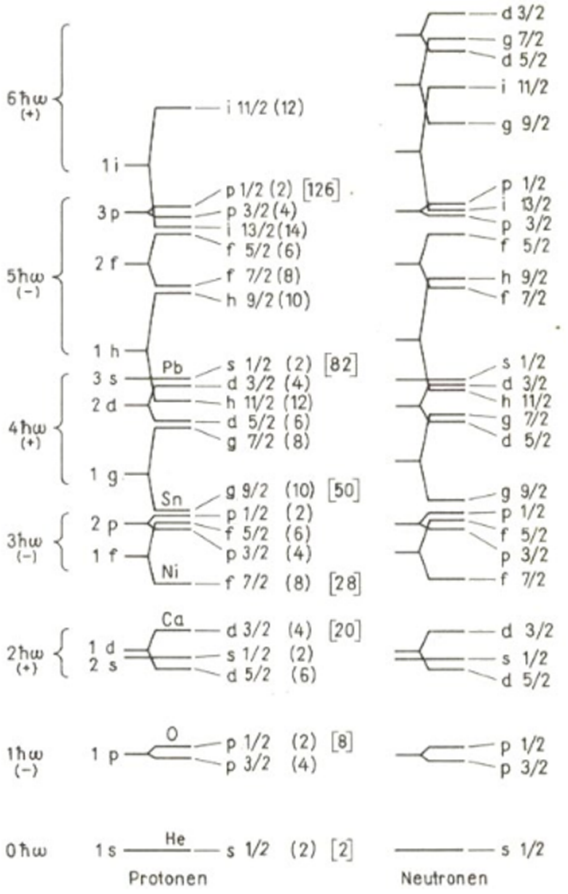

Figure 3: shell model. Source: [4]

2.2.2 Transitions

In the ground state of a nucleus the energetic lowest states are occupied following the Pauli exclusion principle. Similar to the atomic shell the nucleus can be excited. In this excited state one or more nucleons are on energetic higher states. Excited nucleons can emerge as residual product of a radioactive decay or by a electromagnetic excitation. When the nucleon returns to a energetic more favourable state, it has to give up the energy difference. Usually this happens over a γ-radiation and rarer over internal conversion. When a excited atomic shell relaxes, you can only observe dipole radiation. The emission of photons of a higher multipolarity is suppressed and in a case, where this would be necessary, the atomic shell relaxes over other processes than γ-emission. In contrast to the atomic shell the nucleus can't interact as easily with its environment, so you can observe γ-radiation of higher multipolarity. The only competing process is the internal conversion, where the energy is given to an electron in the shell. This process is mainly observed, when the competing photon emission is forbidden or highly suppressed. (see section [2.2.3] and [2.2.4])

2.2.3 Selection Rules

Beside the energy conservation the conservation of the angular momentum and the parity are important. This means that the vectorial subtraction of the angular momentum $\vec{I_i}$ of the initial state and the angular momentum $\vec{I_f}$ of the final state gives the angular momentum $\vec{L}$ of the radiation. This leads to the following possibilities for L:

$$|I_i - I_f| \leq L \leq I_i + I_f \tag{8}$$

While for the magnetic quantum number m (see section [2.1])of the radiation applies:

$$m = m_i - m_f \tag{9}$$

Where m_i and m_f are the magnetic quantum numbers of both states. Additionally applies for photons

$$m \neq 0 \rightarrow L \neq 0 \tag{10}$$

For each angular momentum there are two possible kinds of photon radiation, electric or magnetic. In a classic view this means if a magnetic or electric multipole oscillates. The parity π of these different kinds of radiation are opposed. (see section [2.2.5])

$$\pi_E = (-1)^L$$
$$\pi_M = -(-1)^L$$

Because the parity is a conserved quantity, it has to follow

$$\pi_f = \pi \cdot \pi_i \tag{11}$$

Where π_f is the parity of the final, π_i of the initial state and π the parity of the emitted photon.

2.2.4 Transition Probability

The derivation of the transition probability is very complex, that's why we pass on it. If we assume that there's just one proton which changes its state, we get:

$$P_E(l) = \frac{2(l+1)\omega}{l[(2l+1)!!]^2}\left(\frac{e^2}{\hbar c}\right)\left(\frac{R}{2\pi\lambda}\right)^{2l} S|M_{El}|^2$$
$$P_M(l) = P_E(l) \cdot 10\left(\frac{\hbar}{m_p c R}\right)^2$$

With:

P_E: probability for transition with electric multipole radiation
P_M: probability for transition with magnetic multipole radiation
ω: frequency of the emitted photon
R: Radius of the nucleus

M_{El}: transition matrix element for electric transition
M_{Ml}: transition matrix element for magnetic transition
m_p: mass of a proton
S: statistic factor dependent on I_i,I_f and l, which is normally circa 1

We can see, that the probability is suppressed with greater l and the magnetic transition is more unlikely than the electric transition with same l.

2.2.5 Multipole Radiation

To treat the photon distribution we use the classic description of the photons as a electromagnetic wave. We try to evolve the electromagnetic field by eigenfunctions of the angular momentum because it's a conserved quantity by the transition. We have to solve the Maxwell equations for a source-free room:

$$\vec{\nabla} \times \vec{E} = -\frac{\dot{\vec{B}}}{c}, \qquad \vec{\nabla} \times \vec{B} = \frac{\dot{\vec{E}}}{c} \tag{12}$$

$$\vec{\nabla}\vec{E} = 0, \qquad \vec{\nabla}\vec{B} = 0 \tag{13}$$

$$\tag{14}$$

We use the ansatz of a harmonic oscillating time behaviour of $\exp(-i\omega t)$ and get out of equation(12):

$$\vec{\nabla} \times \vec{E} = ik\vec{B}, \qquad \vec{\nabla} \times \vec{B} = -ik\vec{E}$$

With $k = \frac{\omega}{c}$ From this follows:

$$(\triangle + k^2)\vec{B} = 0 \quad \dot{\vee} \tag{15}$$

$$(\triangle + k^2)\vec{E} = 0 \tag{16}$$

First we first treat the solution of the the scalar equation:

$$(\triangle + k^2)\Phi = 0$$

which are:

$$\Phi_l^m = f_l(kr)Y_{lm}(\theta, \phi) \tag{17}$$

Here is $f_l(kr)$ a pure radial function and Y_{lm} are spherical harmonics, which are eigenfunctions of the angular momentum l and its z-component m. By application of the angular momentum operator $\vec{L} = -i(\vec{r} \times \vec{\nabla})$ on equation(17) we can get solutions for eq (15) & (16)

$$\vec{B}_l^m = f_l\vec{L}Y_{lm}, \quad \vec{E}_l^m = \frac{i}{k}\vec{\nabla} \times \vec{B}_l^m \quad \dot{\vee} \tag{18}$$

$$\vec{E}_l^m = f_l\vec{L}Y_{lm}, \quad \vec{B}_l^m = \frac{-i}{k}\vec{\nabla} \times \vec{E}_l^m \tag{19}$$

The first line describes a electric 2^l-pole field and the second a magnetic 2^l-pole field. These solutions constitute a system by which every solution of the Maxwell equation can be evolved:

$$\vec{E} = \sum_{l,m} [a(l,m) f_l \vec{X}_l^m + b(l,m) \frac{i}{k} \vec{\nabla} \times f_l \vec{X}_l^m]$$

Where $\vec{X}_l^m$ are the normalised vectorial spherical harmonics:

$$\vec{X}_l^m = \frac{\vec{L} Y_l^m}{\sqrt{l(l+1)}}$$

So that the coefficients a and b give the contribution to the respective multipole radiation.

2.2.6 Angular Distribution

The Intensity is described by the absolute value of the Poynting vector:

$$|\vec{S}| = |\frac{1}{\mu_0}(\vec{E} \times \vec{B})|$$

Far away from the source the fields $\vec{B}$ and $\vec{E}$ are approximately orthogonal to each other.

$$|\vec{S}| \approx \frac{1}{\mu_0} E \cdot B = \frac{1}{\mu_0} E^2 = \frac{1}{\mu_0} B^2$$

Because the absolute value of the both fields are the same (see equation (18) & (19)) We are only interested in the angular dependence of the distribution:

$$|\vec{S}| \propto |\vec{X}_l^m|^2 =: Z_l^m(\theta, \phi)$$

$$\rightarrow$$

$$Z_l^m = \frac{1}{2}\left(1 - \frac{m(m-1)}{l(l+1)}\right)|Y_l^{m+1}|^2 + \frac{1}{2}\left(1 - \frac{m(m+1)}{l(l+1)}\right)|Y_l^{m-1}|^2 + \frac{m^2}{l(l+1)}|Y_l^m|^2$$

Example

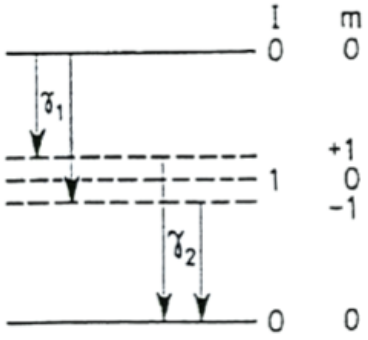

Figure 4: Example of a cascade. Source: [1]

Without a chosen z-axis we have 3 different transitions and therefore the distribution is described by the sum over three different Z_l^m :

$$\begin{aligned} Z_1^{\pm 1} &= \frac{1}{2}\left(\frac{3}{4\pi}\cos^2\theta + \frac{3}{8\pi}\sin^2\theta\right) \\ Z_1^0 &= \frac{1}{2}\frac{3}{4\pi}\sin^2\theta \\ \rightarrow Z_{tot} &= \frac{3}{8\pi} \end{aligned}$$

Which is isotropic like you would expect. But if we chose a z-axis by measuring the first photon, the transition for $m = 0$ disappears and we obtain:

$$W(\theta) = Z_{tot} = 2Z_1^1 = \frac{3}{4\pi}\cos^2\theta + \frac{3}{8\pi}\sin^2\theta = \frac{3}{8\pi}(1+\cos^2\theta)$$

This method can be generalized by group theory (see [5])

$$W(\theta) = \sum_k^K a_{2k}\cos^{2k}\theta \tag{20}$$

With $a_0 = 1$ and $K = \mathrm{Min}\{I_0, l_1, l_2\} \in \mathrm{N}$; I_0 is the middle state of the cascade and $l_{1/2}$ is the angular momentum of $\gamma_{1/2}$. The Anisotropy

$$A = \frac{W(180°)}{W(90°)} - 1 = \sum_{i=1}^{2} a_i \tag{21}$$

is a measurement for the diviation of the isotropy.

If I_0 is not an integer $I_0 - \frac{1}{2}$ is used. The coefficients a_{2k} are determined for some cascades:

γ-γ cascade $I_A(l_1)I_B(l_2)I_C$	$W(\vartheta)\,d\Omega = (1 + a_2\cos^2\vartheta + a_4\cos^4\vartheta)\,d\Omega$	
	a_2	a_4
0(1)1(1)0	1	0
1(1)1(1)0	$-\frac{1}{3}$	0
1(2)1(1)0	$-\frac{1}{3}$	0
2(1)1(1)0	$-\frac{1}{3}$	0
3(2)1(1)0	$-\frac{3}{29}$	0
0(2)2(2)0	-3	$+4$
1(1)2(2)0	$-\frac{1}{3}$	0
2(1)2(2)0	$+\frac{3}{7}$	0
2(2)2(2)0	$-\frac{15}{13}$	$+\frac{16}{13}$
3(1)2(2)0	$-\frac{3}{29}$	0
4(2)2(2)0	$+\frac{1}{8}$	$+\frac{1}{24}$

Figure 5: Correlation coefficients (source: [2])

2.3 Used Probes

For the energy calibration we used Cobalt-60 and Sodium-22 and their known spectrum.

Sodium-22:
Sodium decays to nearly 89.9% over β^+-decay and to 10.1% over electron catch to an excited state of Neon:

$$^{22}_{11}Na \rightarrow ^{22}_{10}Ne^* + e^+ + \nu_e$$
$$^{22}_{11}Na + e^- \rightarrow ^{22}_{10}Ne^* + \nu_e$$

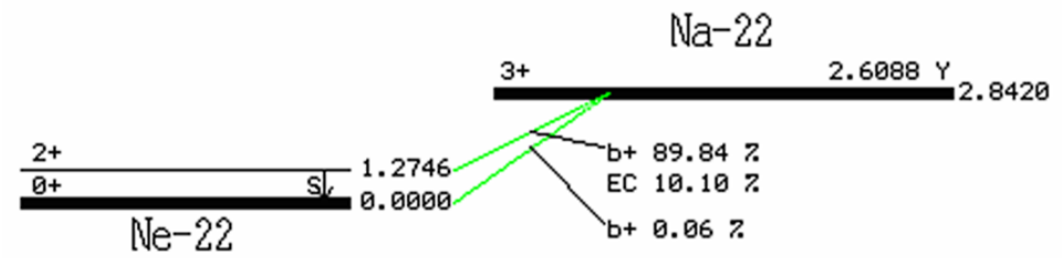

Figure 6: Decay of Na-22.(Source: [7])

So we can detect two peaks in the Na-spectrum. One from the transition into the ground state (1274.6keV) and one from the electron-positron-annihilation (511keV = electron mass)

Cobalt-60:
Cobalt decays nearly to 100% over β^--decay to the third excited state of Nickel:

$$^{60}_{27}Co \rightarrow ^{60}_{27} Ni + e^- + \overline{\nu}_e$$

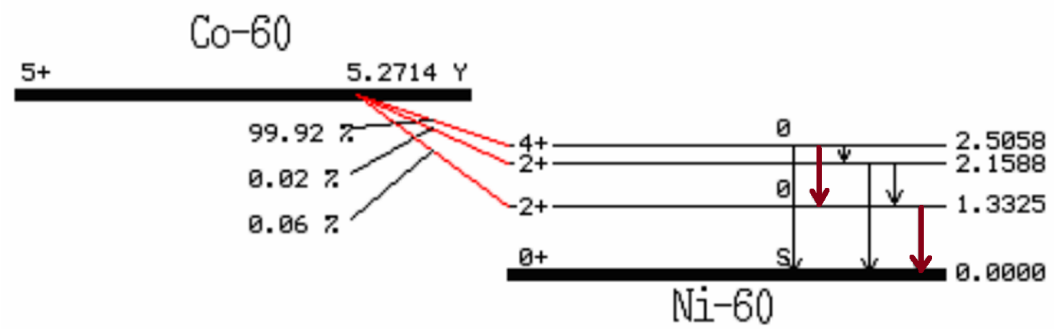

Figure 7: Decay of Co-60.(Source: [7])

This excited state transitions mainly to the first excited state and this transitions to the ground state.So we can see again two peaks at 1173.2keV and at 1332.5keV (see image(7))

Rhutenium-106 We use Ruthenium-106 to produce excited states of Palladium:

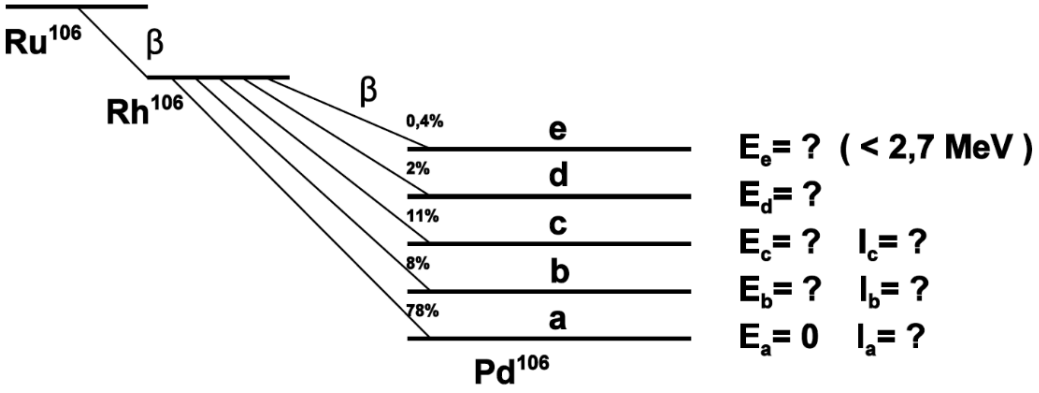

Figure 8: Simple decay sheme of Ru-106.(Source: [1])

We try to find the in the image listed values in our experiment.

III Procedure

3.1 Set-Up

The Set-Up of the experiment is really simple. We have two detectors: one fixed on a point of a circle around a probe and the other one can be moved on this circle. With the detectors we can count coincidences for every angle between them.

3.1.1 Devices

To execute the experiment, we need a selection of electronic devices which we want specify and explain their functions.

Scintillation Counter
The scintillation counter converts a γ-quantum into an electronic impulse. The physical effects responsible for the conversion are the photo effect and compton scattering. So with a scintillation counter it is possible to make γ-quanta countable.

Amplifier
The Amplifier simply amplifies the signal and has a uni -and bipolar output.

Single Channel Analyzer
The SCA operates like a Band-Pass-Filter for voltages. You can set the width of the band and the start of the band. In contrast to the real Band-Pass-Filter, the SCA only emits a single well defined signal with the same shape for every voltage that is in the allowed band.

Multi Channel Analyzer
The MCA works in principle the same way as the SCA. The only difference is, that you can't define a 'window' in which it passes a signal and the signal is split up in 1024 channels ordered by the height of the signal. Each channel represents a little voltage interval. Connected to a computer the MCA shows you a full spectrum of the input voltage.

Linear Gate
The Linear Gate has a enable-input and a normal input. The output of the linear gate is just the normal input at the time it gets an enable signal.

Fast Coincidence Device
The Fast Coincidence Device gives a signal, if two or more signals are registered within the selectable resolving time.

Linear Mixer, 50Hz Clock and Hex-Scaler
These simple devices aren't as important as the other ones but they are needed to make the experiment work. The Hex-Scaler simply counts the input signals. The 50Hz Clock is used for time measurement because it counts by a frequency of 50Hz as long as we count the coincidences. And the linear mixer is just used to reverse the signal of the coincidence device from a positive signal to a negative signal because the Hex-Scaler just counts on negative signals.

3.1.2 Energy Calibration

For the energy calibration measurement we simply connected the scintillation counters with the amplifier and than the uni polar output of the amplifier with the multi channel analyzer which is connected to a computer.

3.1.3 Energy Windows

To set the energy windows for every decay, we had to combine the SCA and the MCA. By giving the amplified signal to the linear gate and the SCA, we could use the output of the SCA as enable signal. So the MCA only gets the signals, that can pass through the SCA. In the drawing below you can see the set up for setting the windows of SCA 1 (orange) and SCA 2 (yellow). Of course they can't be realized at the same time.

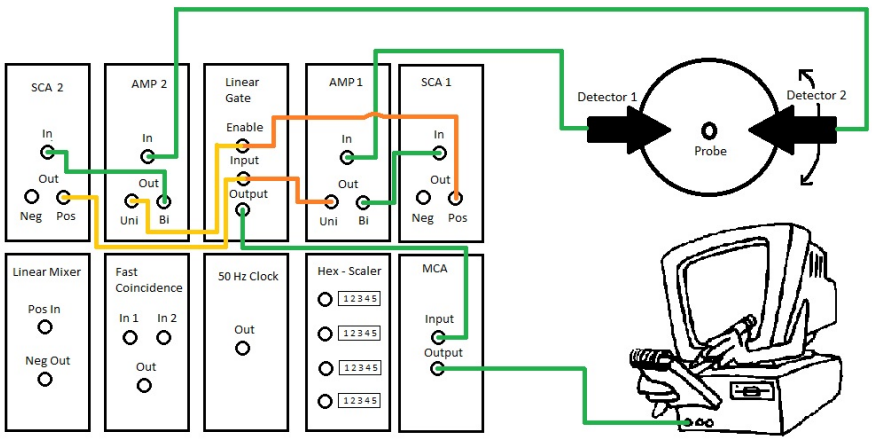

Figure 9: Set-Up for setting the energy windows

3.1.4 Coincidences

For the measurement of the coincidences, we don't need the MCA, because we can simply use the Hex-Scaler to count the coincidences, the events from the scintillation counters and the time.
That's why we don't use the linear gate as well. We use both outputs of the SCAs, one for counting with the Hex-Scaler and the other one to measure the coincidences. The output of the coincidence device must be inverted by the linear mixer, because the Hex-Scaler needs a negative input signal. Finally we

use the 50Hz clock to measure the time. We can either stop the counting by defined number of counts of the 50Hz clock or we just use the count of the 50Hz clock to get the elapsed time.

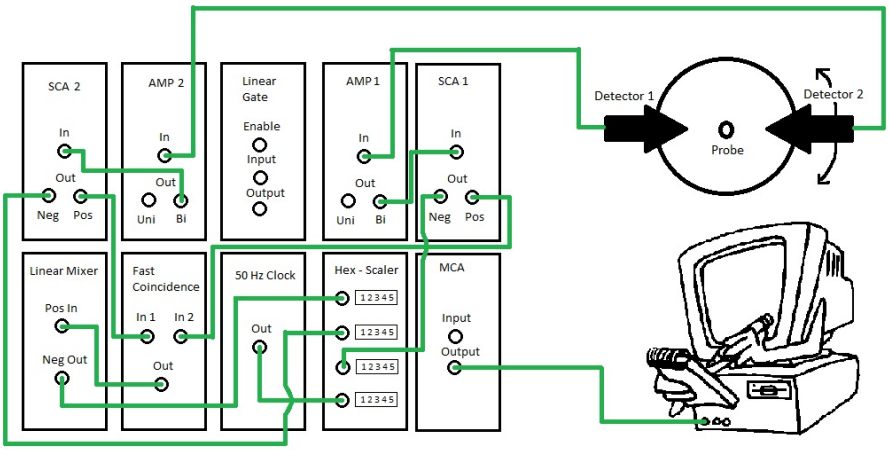

Figure 10: Set-Up for the coincidence measurement

3.2 Energy Calibration

We measured the Spectrum of Cobalt and Sodium with the moveable detector (D2) and adjusted the amplifier, so that the last peak of Cobalt (1332.5keV) was seen a little bit under channel 800. This way we could be sure to have linear amplifying in the interesting energy area. We measured the spectra each for circa 40min. Then we measured the spectrum of Palladium with the same amplifier settings for about 20min.

3.3 Delay

For the coincidence measurement we needed to adjust a delay between the two SCA. We used the 511keV peak of sodium to determine the delay settings. We know that this peak is caused by the positronium decay which sends two photons in opposite directions. First we had to choose the energy window for the measurement. We set the window for each detector at the peak of 511keV. Then we set the detectors with a angular of 180° between each other and used the coincidence set-up. We set the delay of the SCA2 of the second detector D2 to a fixed value ($d = 0.06\mu$s) and variegated the delay of the SCA1 of the first delay. For the rough delay setting we used the oscilloscope and tried to match the observed pulses. We measured the coincident counts N_c as a function of the delay and chose the delay of maximal counts as delay for our measurement with palladium. The rate fluctuated a lot so we measured the chosen point more than once to be sure to have chosen a good operating point. We could use the same delay for palladium as for sodium, although the positron and electron are emitted simultaneously, because the life time of the middle state of the γ-γ-decay is short enough to be seen as simultaneously as well.

3.4 Angular Resolution

To determine the angular resolution of the detector we use again the positronium decay of sodium. We use the coincidence set-up and measure the counts as function of the angular with set energy windows. Because we don't know how the sodium is put in the given plastic stick we can't know how centred it is between the two detectors. So we variegate the position of the probe and measure multiple series to compare the width of the resulting Gaussian curves.

3.5 Angular Distribution

We set the energy windows of the two detectors to the peaks we identified as the two peaks related by the γ-γ-cascade we're interested in. We use the movable detector D2 for the second peak of the decay (in the spectrum it is the higher one because beside the γ-γ-cascade it can appear as usual γ-decay to the ground state).
First we measured from 70° to 290° in $\Delta\alpha = 10°$ steps with a time of approximately 3 minutes. We set the Hex-Scaler to stop at 10000 counts from the 50Hz Clock. With this data we could get a feeling for the analysis, but with this short measurement period the statistics are to bad to get a significant result. So we did the measurement again. This time we didn't use the 50Hz clock to stop the measurement, but we used it to measure the time. We did $\Delta\alpha = 20°$ steps from 70° to 290° and then again from 80° to 280° with a measuring time of about 10 minutes per step. The data we took from this measurement was good, but since we had 2 weeks to measure we figured that we could do better.
So we started again with smaller energy windows and again $\Delta\alpha = 20$ degree steps from 70° to 290° and then from 80° to 280°. This time we measured each step for about 20 minutes. Since this measurement takes up to 7 hours and 40 minutes of pure measuring time, we thought we could split it up to 2 days, if we won't touch the setup over night. Sadly the data shows, that, even without touching, something changed over night and the points we measured the second day had a lower count rate than the day before:

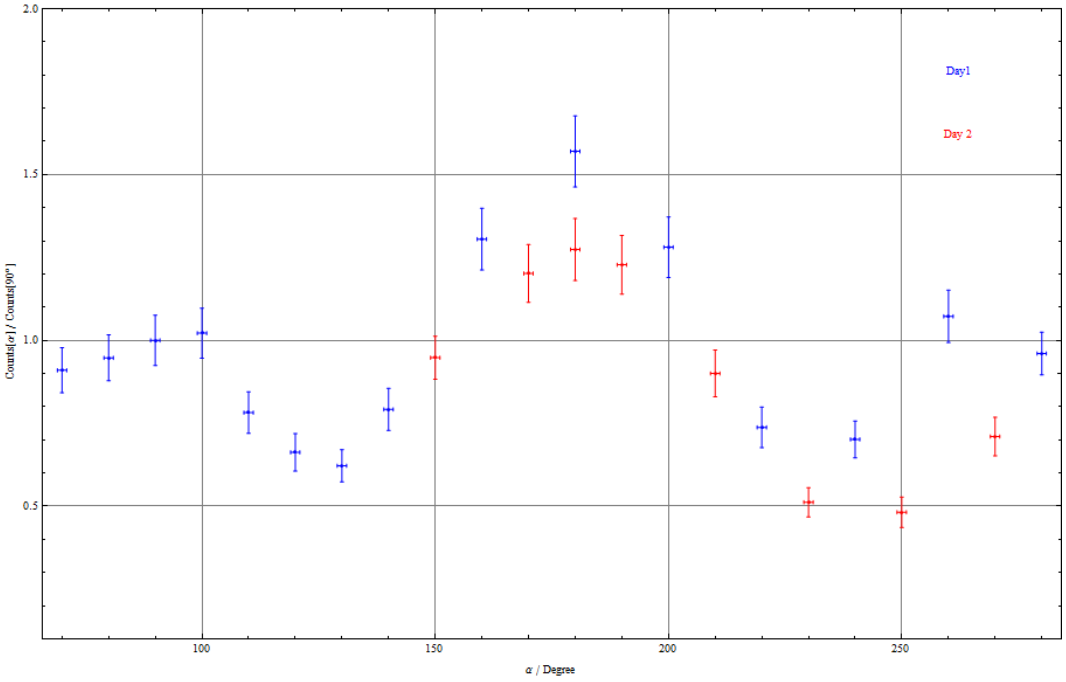

Figure 11: Third measurement - Day 1 and Day 2

Obviously something had changed over night and to prove it, we measured the 180° point again. We can't say for sure what the problem was, but we think the window settings of the SCAs changed. That's why we couldn't use the data and had to measure again.
First we set the energy windows again and then we measured in $\Delta\alpha = 10°$ steps for 20 minutes again. But this time we started at 180 degree and measured by turns $180° + n \cdot \Delta\alpha$ and $180° - n \cdot \Delta\alpha$ (n = 0,1,2,...,11), so that a changing of the energy windows (or what ever caused the problem) was effecting to both sides equally.

IV Analysis

4.1 Delay

For the Counts in respect to the delay we measured:

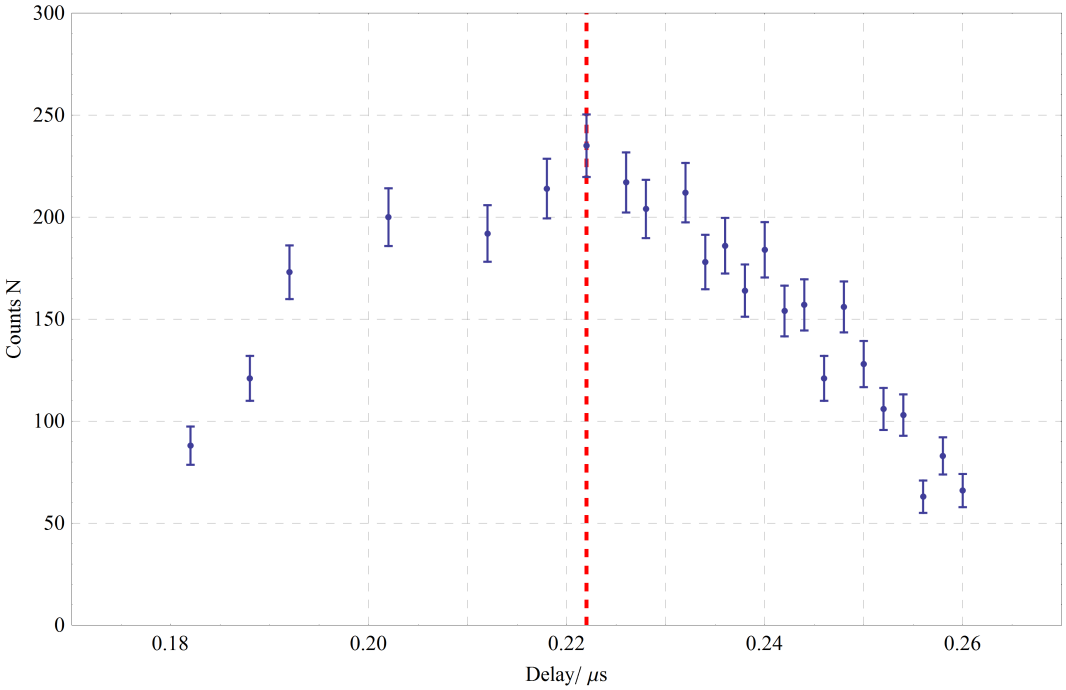

Figure 12: Counts in respect of the delay

We chose the marked point for our measurement with palladium: delay = 0.222μs
We measured this point several times to be sure to be at a maximum.

4.2 Energy Calibration & Energy Spectrum

We fitted the sum of two Gaussian functions and a exponential function to the two peaks of the cobalt spectrum with Mathematica, because the two peaks are very close to each other. The Fit was done with weights $w_i = 1/s_i^2$ where $s_i = \sqrt{N_i}$ is the uncertainty of the Counts N_i The fit function has therefore the form:

$$f_c(x) = \frac{h_1}{s_1} \cdot \mathrm{Exp}\left[-0.5 \cdot \left(\frac{x - m_1}{s_1}\right)^2\right] + \tag{22}$$

$$\frac{h_2}{s_2} \cdot \mathrm{Exp}\left[-0.5 \cdot \left(\frac{x - m_2}{s_2}\right)^2\right] + \tag{23}$$

$$a \cdot \mathrm{Exp}[e \cdot x] + c \tag{24}$$

We got the parameter values:

	Value x	Standard Error s_x
m_1	744.9	1.0
m_2	659.5	0.7
h_1	38000	1000
s_1	42.23	0.7
h_2	27600	1200
s_2	30.6	0.8
c	54	5
e	130000	20000
a	0.0081	0.0003

(25)

With the fit curve:

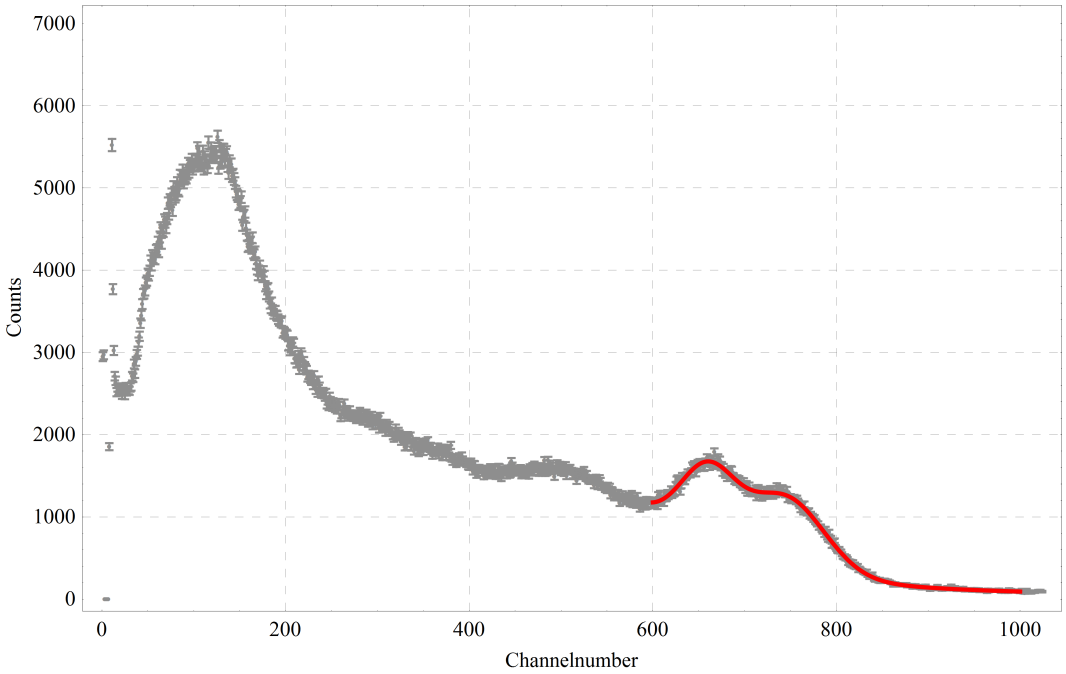

Figure 13: Spectrum Cobalt

For this fit curve we calculated the $\frac{\chi^2}{DoF}$ with:

$$\chi^2 = \sum_k \left(\frac{N_{mess\ k} - N_{Theo\ k}}{s_{Nmess\ k}} \right)^2 \tag{26}$$

Where the sum goes over all used measured value. Which gives

$$\frac{\chi^2}{DoF}\,(Co) = 1.03$$

We fitted to each peak of the Sodium spectrum the sum of a single Gaussian function and a exponential function. We used the following fit function for both peaks:

$$f_s(x) = \frac{h}{s} \cdot \mathrm{Exp}\left[-0.5 \cdot \left(\frac{x-m}{s} \right)^2 \right] + \tag{27}$$

$$a \cdot \mathrm{Exp}[e \cdot x] + c \tag{28}$$

And got the values for the parameters:

	Value x	Standard Error s_x
m_1	302	0.2
h_1	−26000	300
s_1	−19.6	0.2
c_1	30	30
e_1	3250	150
a_1	0.0057	0.0003
m_2	726.8	1.1
h_2	4170	150
s_2	36.9	1.2
c_2	−23	3
e_2	1800	70
a_2	0.00381	0.00011

(29)

With the fit curve:

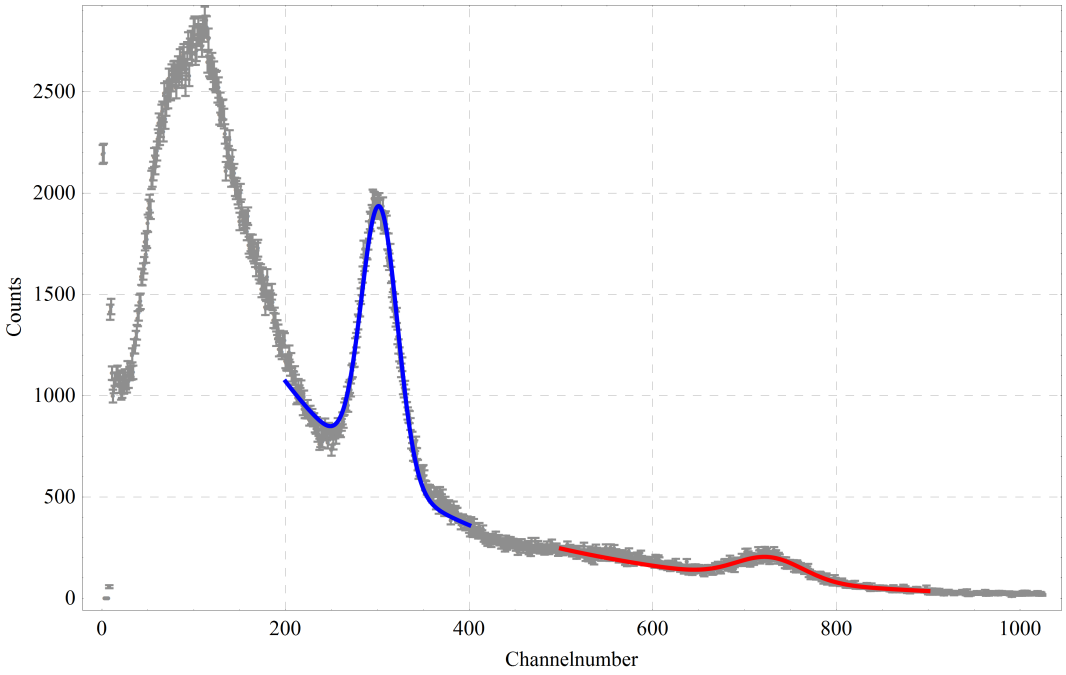

Figure 14: Spectrum Sodium (Blue: Peak with parameters 1 , Red: Peak with parameters 2)

And their $\frac{\chi^2}{DoF}$:

$$\frac{\chi^2}{DoF}(Na1) = 2.80$$
$$\frac{\chi^2}{DoF}(Na2) = 2.53$$

We know the spectrum of Sodium and Cobalt (see section [2.3]).
Their peaks are ate 511keV and 1274.6keV for Sodium and 1173.2keV and 1332.5keV for Cobalt.

With these energy values we could calibrate the MCA, which works linear in the chosen area. We used a linear fit:

$$E(m) = a \cdot m + c \tag{30}$$

Where Ch is the channel position of the peaks and also the parameter m of the fitted curves. With Mathematica we got the parameter values with their uncertainties:

	Value x	Standard Errors$_x$
c	-44	12
a	1.84	0.02

(31)

And the linear slope:

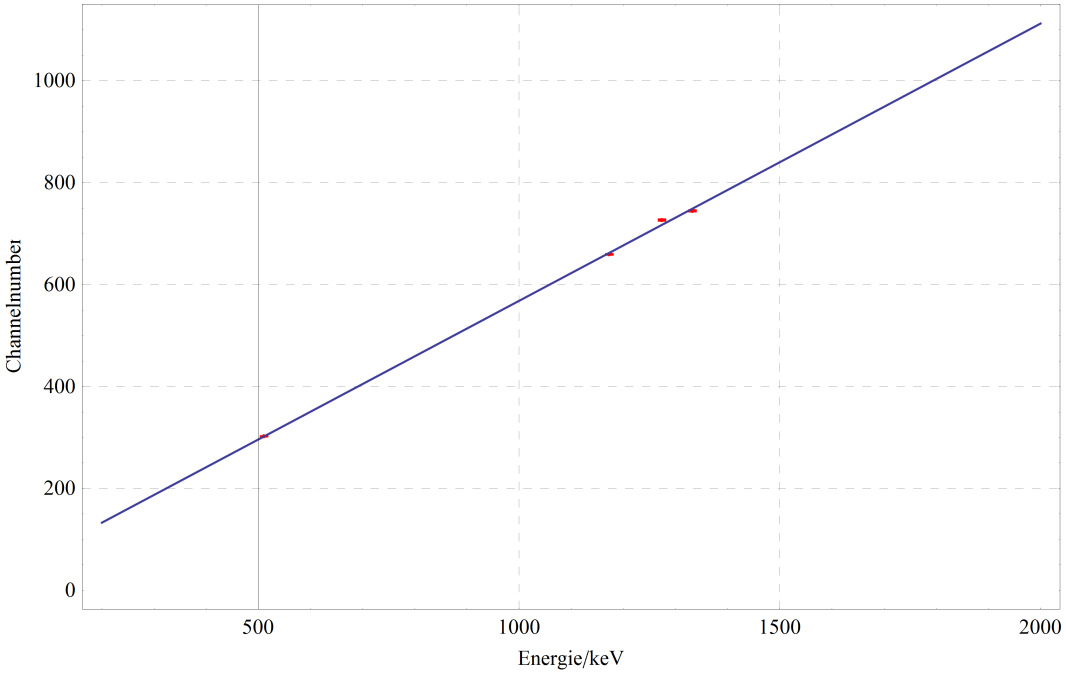

Figure 15: Energy calibration (The errorbars are too small to be seen in this graph, see table(25) & (29))

We used the same way to find the peak positions in the measured Palladium spectrum as we used for the Cobalt and Sodium spectrum. We fitted the curve (22) to the double peak and the curve (27) to the single one. This way we got

the following parameters with their uncertainties:

	Value x	Standard Error s_x
m_1	303.17	0.09
m_2	361.8	0.3
h_1	722000	4000
s_1	19.54	0.07
h_2	431000.	4000
s_2	28.12	0.19
c_{12}	3090	40
e_{12}	223000.	8000
m_3	621.0	0.5
h_3	40700	1500
s_3	40.7	0.8
c_3	−110	50
e_3	80000	10000

(32)

With the fit curves:

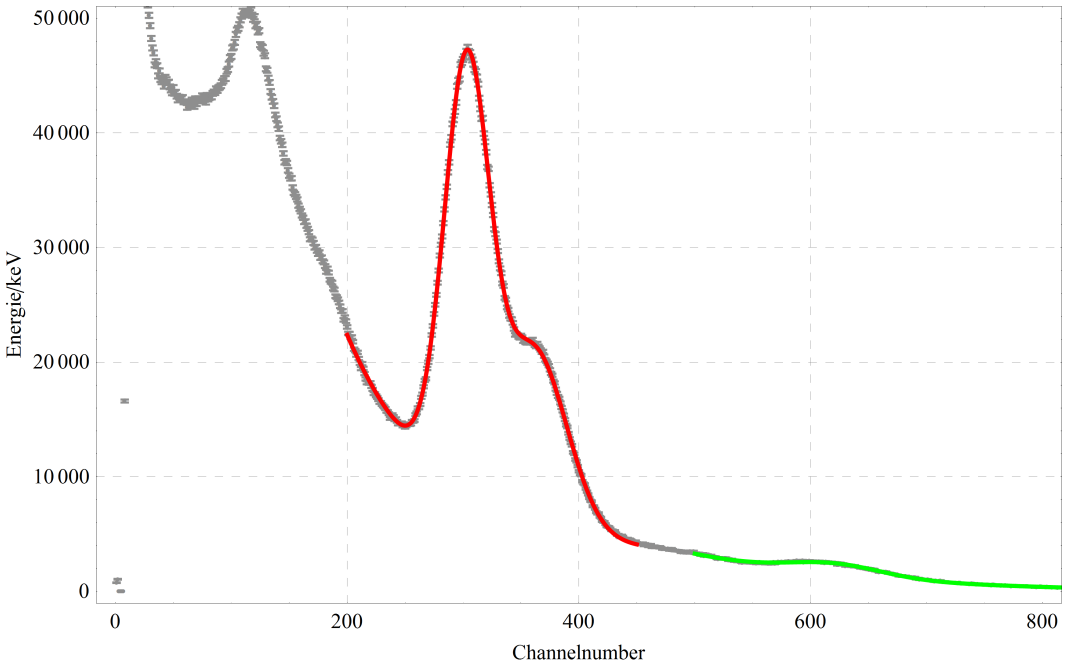

Figure 16: Palladium spectrum (Red: Double peak with parameters 1 and 2, Green: Single peak with parameters 3)

and their $\frac{\chi^2}{DoF}$:

$$\frac{\chi^2}{DoF}(Pd12) = 3.49$$
$$\frac{\chi^2}{DoF}(Pd3) = 1.56$$

We used the resulted linear fit equation (30)

$$E(m) = a \cdot m + c \tag{33}$$

with a and c out of the parameter table (31) to calculate the Energies of each peak. The errors of these energies are calculated by error propagation of each parameter (s_a and s_c , also found in table (31)) and the channel positions m with their errors s_m (see table (32)) :

$$s_E = \sqrt{m^2 \cdot s_a^2 + a^2 \cdot s_m^2 + s_c^2} \tag{34}$$

With these equations we got following values for the three found peaks in the spectrum of Palladium:

i	E_i/keV	s_i/keV
1	513	14
2	620	15
3	1097	19

(35)

We can see that the first two energy peaks sum up to the third one. That means that these first two peaks are related over a γ-γ-cascade.

4.3 Angular resolution

As described before, we measured the angular resolution and fitted the data with a gaussian-function:

$$f(x) = \frac{a_1}{a_3} \cdot e^{-\frac{1}{2}\cdot\left(\frac{x-a_2}{a_3}\right)^2} \tag{36}$$

To see the goodness of the fit we also determined χ^2:

$$\chi^2 = \sum \left(\frac{y_i - f(x_i)}{\sigma_{y_i}} \right)^2 \tag{37}$$

For the first three measurements, with the probe centered as good as possible, we got the following results.

4.3.1 Measurement 1 - 3

Measurement 1

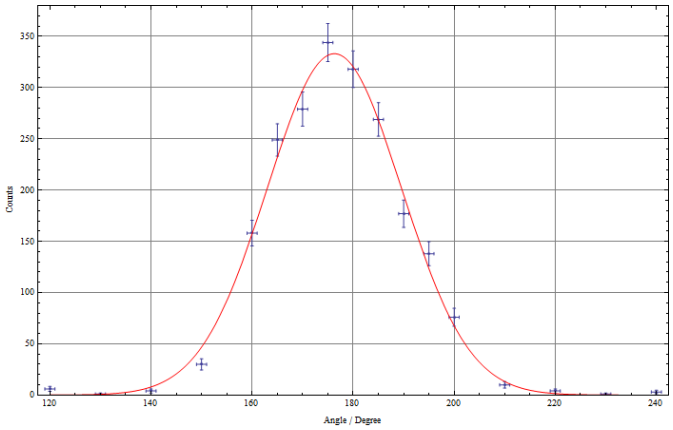

Figure 17: angular resolution #1

#1	Estimate	Standard Error
a1	4420	94
a2	176.3	0.3
a3	13.3	0.3

$\chi^2 = 33.0245$

Measurement 2

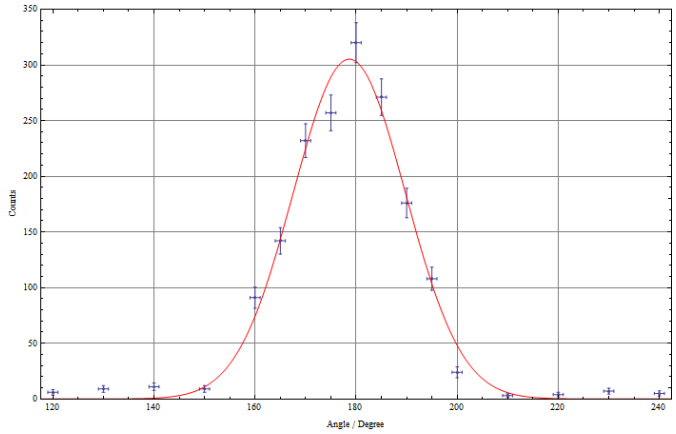

Figure 18: angular resolution #2

#2	Estimate	Standard Error
a1	3387	99
a2	178.7	0.4
a3	11.1	0.4

$\chi^2 = 75.7416$

Measurement 3

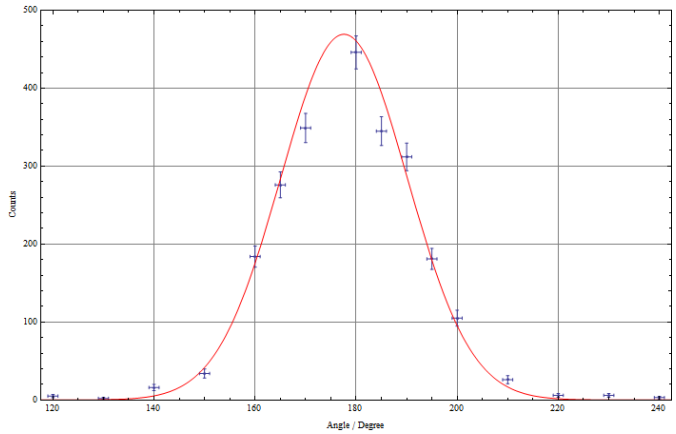

Figure 19: angular resolution #3

#3	Estimate	Standard Error
a1	5884	223
a2	177.6	0.5
a3	12.5	0.6

$\chi^2 = 57.4437$

As you can see easily the Gaussian function is shifted from the 180° by a few degrees and the width is varying as well. So we determined the weighted

mean of the width a_3 because that's the parameter we're interested in.

$$\overline{a_3} = \frac{\sum_1^3 \frac{a_{3,i}}{\sigma^2_{a_{3,i}}}}{\sum_1^3 \frac{1}{\sigma^2_{a_{3,i}}}} = 12.4 \tag{38}$$

$$\sigma_{\overline{a_3}} = \frac{1}{\sum_1^3 \frac{1}{\sigma^2_{a_{3,i}}}} = 0.2 \tag{39}$$

But we didn't know, if the value of a_3 was effected by the shift of a_2 from 180°, so we did two measurements with the probe positioned off-center as much as possible.

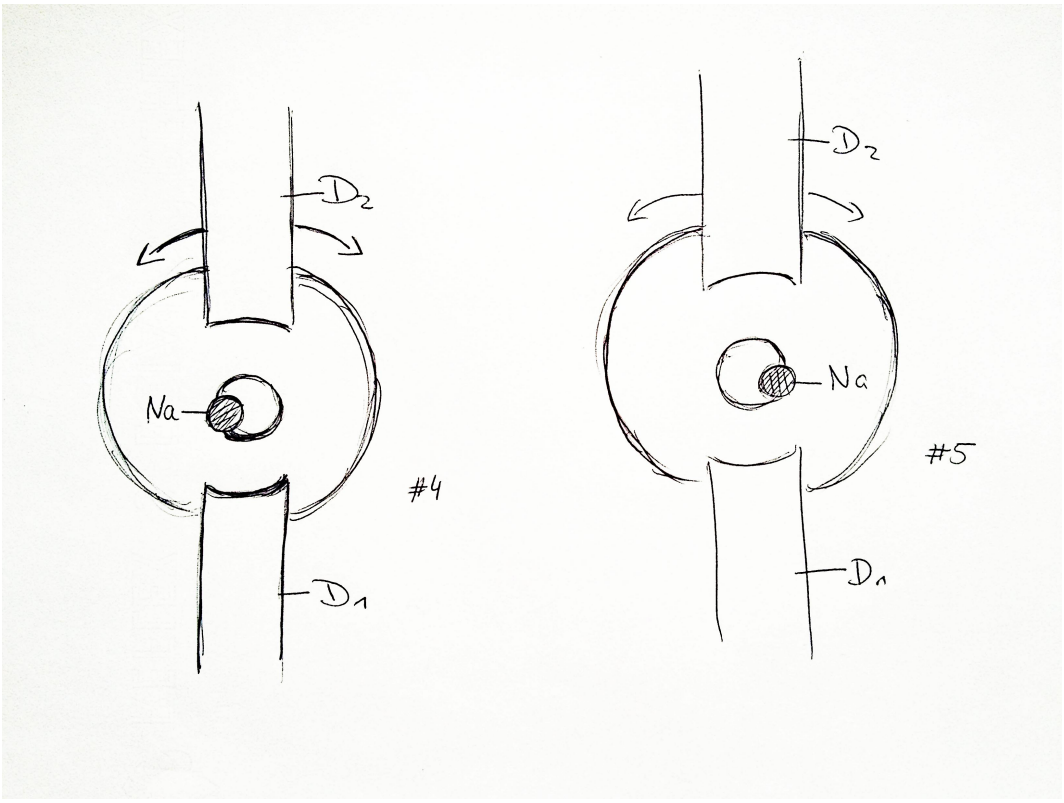

Figure 20: probe position in 4 and 5

4.3.2 Measurement 4 and 5

Measurement 4

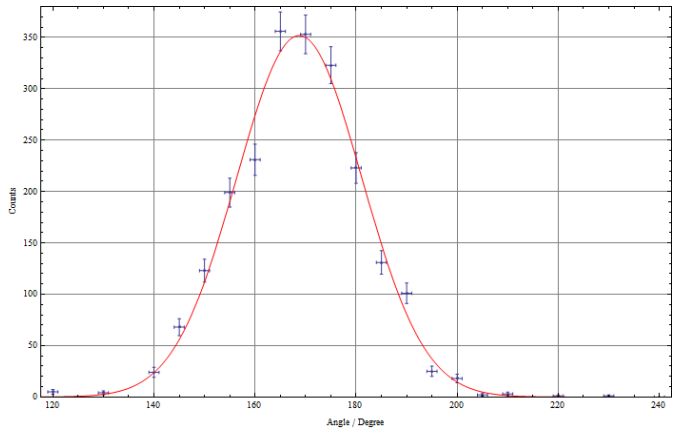

Figure 21: angular resolution #4

#4	Estimate	Standard Error
a1	4355	109
a2	168.7	0.4
a3	12.4	0.4

$\chi^2 = 38.6673$

Measurement 5

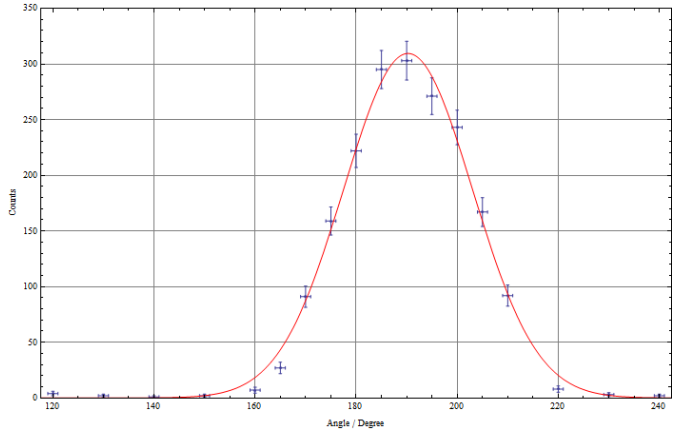

Figure 22: angular resolution #5

#5	Estimate	Standard Error
a1	3941	72
a2	190.3	0.3
a3	12.7	0.3

$\chi^2 = 59.1779$

With these measurements we could see, that the width of the Gaussian function doesn't really depend on the position of the probe in our set-up. Of course it always does a little, because of the geometry, but in our set-up the effects are insignificant. That's why we decided to determine the weighted mean over all 5 measurements to get the value of a_3.

$$\overline{a_3} = \frac{\sum_1^5 \frac{a_{3,i}}{\sigma^2_{a_{3,i}}}}{\sum_1^5 \frac{1}{\sigma^2_{a_{3,i}}}} = 12.5 \tag{40}$$

$$\sigma_{\overline{a_3}} = \frac{1}{\sum_1^5 \frac{1}{\sigma^2_{a_{3,i}}}} = 0.2 \tag{41}$$

4.4 Angular Correlation

4.4.1 Random coincidences

We measured the random coincidences over night by setting the delay of SCA2 to a very high value (7.14 μs), so that there is no chance of a real coincidence. We measured the following values:

Event	Counts
Random Coincidences	435
$t \cdot 50Hz$	869822

(42)

So we got the counting rate of

$$N_{random} = \frac{435 \cdot 50}{869822} \frac{1}{s} = 0.025 \frac{1}{s} \tag{43}$$

with the statistical error of:

$$\sigma_{N_{random}} = \frac{\sqrt{435} \cdot 50}{869822} \frac{1}{s} = 0.001 \frac{1}{s} \tag{44}$$

But with a relative error of

$$\frac{\sigma_{N_{random}}}{N_{random}} = 0.048 \tag{45}$$

we can can disregard the error in the following error propagation.

4.4.2 Angular Distribution

We measured the angular distribution as mentioned before. And Just like the random coincidences we determined the counting rates for each angular. The next step was to norm the data to the 90° point and subtract the random coincidences:

$$N_{norm,i} = \frac{N_i - N_{random}}{N_{90°} - N_{random}} \tag{46}$$

And the error:

$$\sigma_{N_{norm,i}} = N_{norm,i} \cdot \sqrt{\left(\frac{N_i}{\sigma_{N_i}}\right)^2 + \left(\frac{N_{90°}}{\sigma_{N_{90°}}}\right)^2} \tag{47}$$

In theory we should see the angular distribution

$$W(a_1, a_2, \Theta) = 1 + a_1 \cdot cos(\Theta)^2 + a_2 \cdot cos(\Theta)^4. \tag{48}$$

But with the finite aperture angle and the resulting angular resolution we can't fit this function on our data. We have to convolve the theoretical angular distribution with a Gaussian function

$$G(x, \Theta, \sigma) = \frac{1}{\sqrt{2 \cdot \pi} \cdot \sigma} \cdot e^{-\frac{1}{2} \cdot \left(\frac{x - \Theta}{\sigma}\right)^2} \tag{49}$$

with the width σ we determined before from the angular resolution:

$$g(x) = \int W(a_1, a_2, \Theta) \cdot G(x, \Theta, \sigma) d\Theta \tag{50}$$

But since we couldn't fit this function to our data, because of the integral, we summed over 360° in 1° steps and because we didn't measure the 90° more exactly for the normalization, we added a new parameter h_1 to adjust the error in normalization on the other parameters:

$$\widehat{g}(x) = h_1 \cdot \sum_{\Theta=0}^{360} W(a_1, a_2, \Theta) \cdot G(x, \Theta, \sigma) \tag{51}$$

To appraise the errors on the parameters we didn't just looked at the error given by the fit, we also wondered how significant the difference of the parameters were if we added/subtracted the error on the width of the Gaussian function from the angular resolution. So fitted the data three times.

Fit 1

$$\widehat{g_1}(x) = h_1 \cdot \sum_{\Theta=0}^{360} W(a_1, a_2, \Theta) \cdot G(x, \Theta, \sigma - s_\sigma) \tag{52}$$

	Estimate	Standard Error
h1	1.13042	0.0365419
a1	−2.81568	0.146575
a2	3.35706	0.163202

$\frac{\chi^2}{dof} = 27.55$

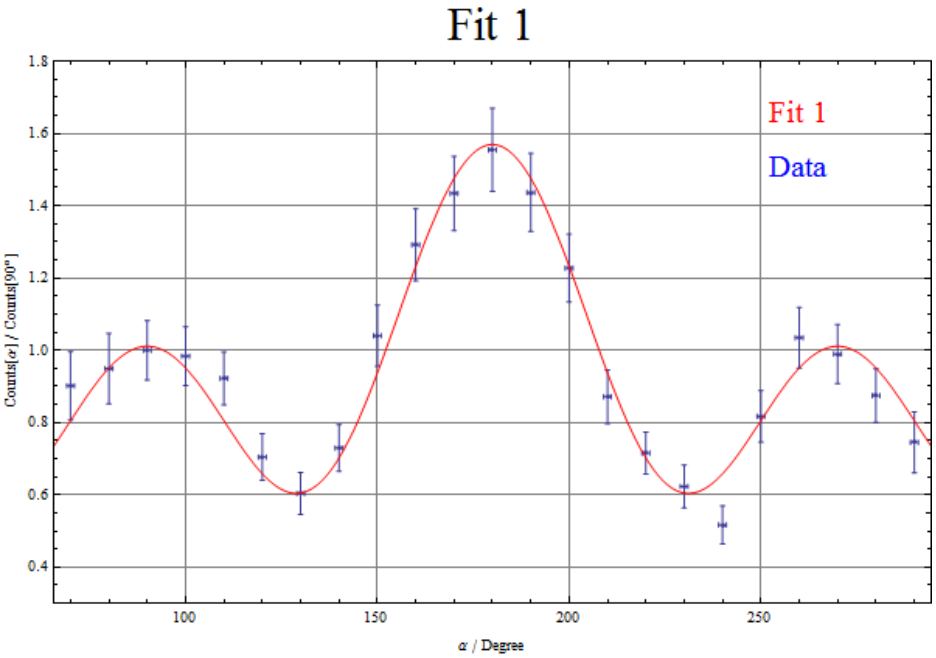

Figure 23: angular distribution - fit1

Fit 2

$$\widehat{g_2}(x) = h_1 \cdot \sum_{\Theta=0}^{360} W(a_1, a_2, \Theta) \cdot G(x, \Theta, \sigma) \tag{53}$$

	Estimate	Standard Error
h1	1.13527	0.0368502
a1	−2.84269	0.147156
a2	3.38339	0.163777

$\frac{\chi^2}{dof} = 26.99$

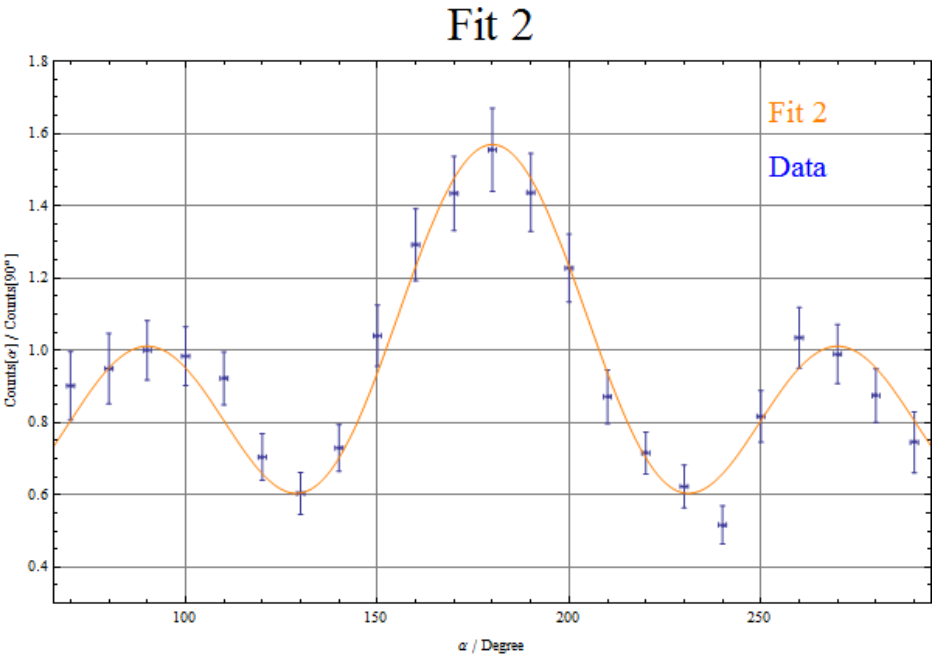

Figure 24: angular distribution - fit2

Fit 3

$$\widehat{g_3}(x) = h_1 \cdot \sum_{\Theta=0}^{360} W(a_1, a_2, \Theta) \cdot G(x, \Theta, \sigma + s_\sigma) \tag{54}$$

	Estimate	Standard Error
h1	1.14026	0.0371683
a1	−2.87022	0.147736
a2	3.41022	0.164349

$\frac{\chi^2}{dof} = 26.45$

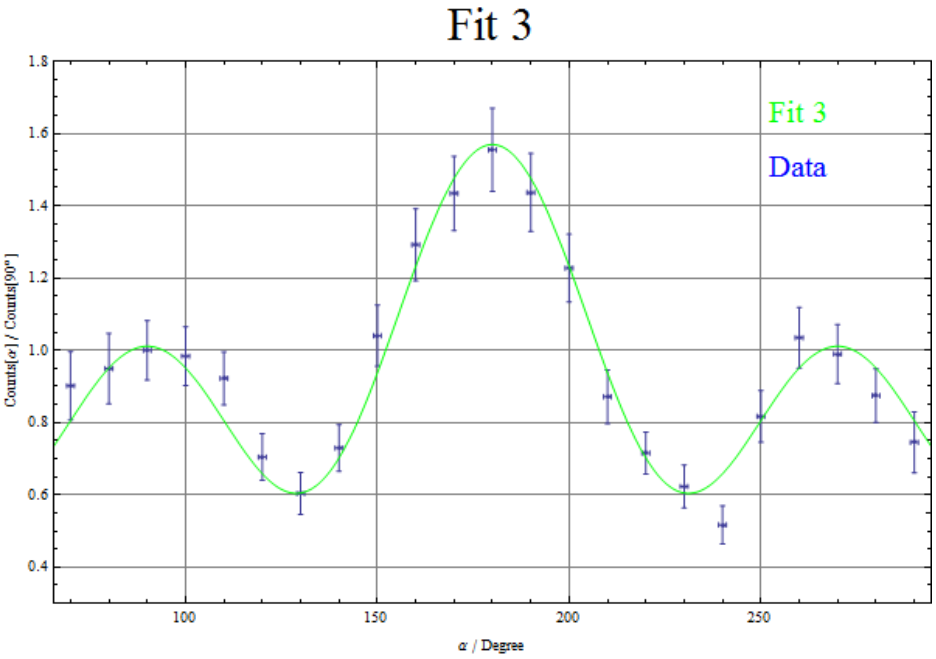

Figure 25: angular distribution - fit3

As you can see the differences caused by the error of the Gaussian width Δa_i is very small and disappears within the error of the fit parameters:

Parameter	Δa_i	Mean Standard Error
a1	0.055	0.147
a2	0.053	0.164

So we think its reasonable to disregard the error of the Gaussian width and just go with errors of the fit.

As you remember, while measuring the angular resolution, we saw that the measured Gaussian function was shifted in middle by about 2.5°. But since the geometry of the probe used for the angular resolution was different from the one we used to measure the angular distribution, we wont correct the data, but see what effect a shift of 2.5° has on the fit parameters. So once again we defined a slightly alternated fit function

$$\widehat{g_4}(x) = h_1 \cdot \sum_{\Theta=0}^{360} W(a_1, a_2, \Theta) \cdot G(x + 2.5, \Theta, \sigma) \tag{55}$$

	Estimate	Standard Error
h1	1.12817	0.0407287
a1	−2.81664	0.164064
a2	3.36497	0.181812

$\frac{\chi^2}{dof} = 26.95$

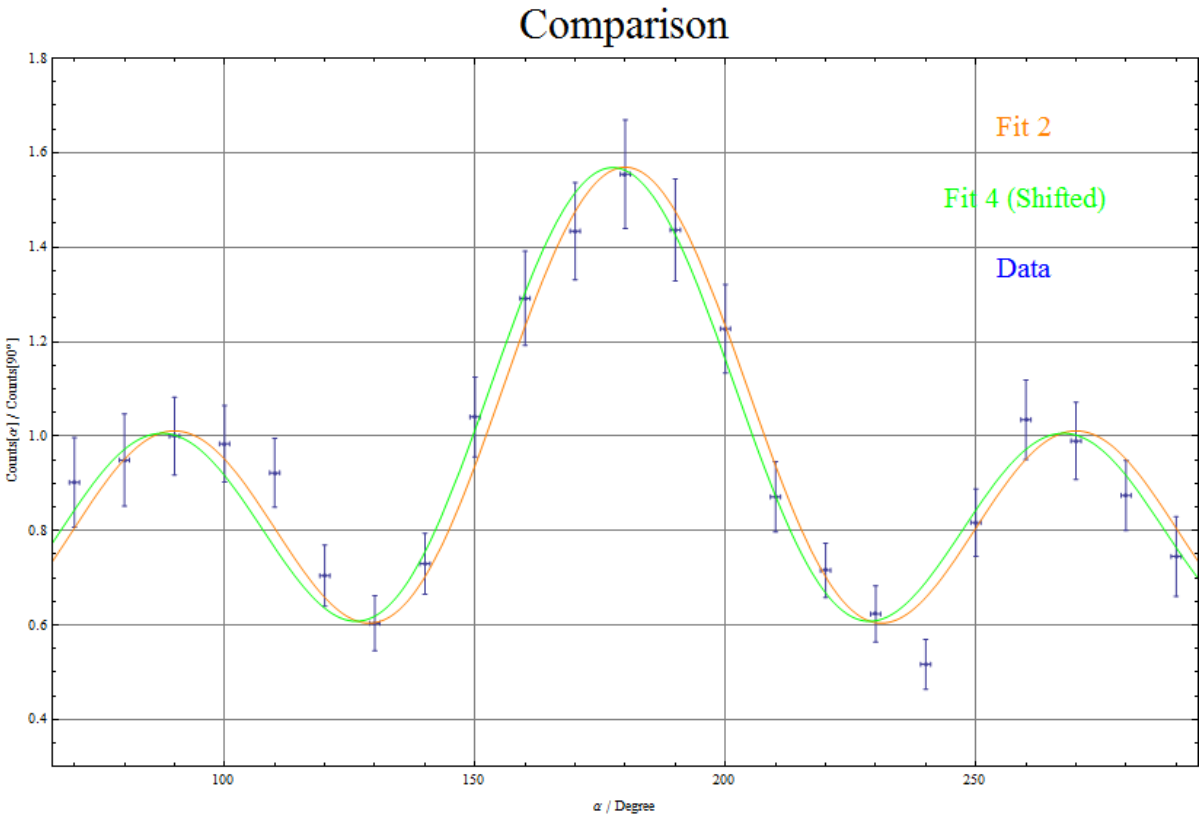

Figure 26: Comparison - fit2 & fit4

Again the difference in the parameters Δa_i isn't very big:

Parameter	unshifted fit2	shifted fit4	Δa_i
a1	−2.84	−2.82	0.02
a2	3.38	3.36	0.02

So we probably won't have large effects from the shift and we can use the second fit to get the parameters and end up with the angular distribution

$$W(\Theta) = (1.14 \pm 0.04) \cdot \left(1 + (-2.84 \pm 0.15) \cdot cos(\Theta)^2 + (3.38 \pm 0.16) \cdot cos(\Theta)^4\right) \tag{56}$$

With this we can determine the anisotropy

$$A = \frac{W(180°)}{W(90°)} - 1 = \sum_{i=1}^{2} a_i = 0.54 \tag{57}$$

And its error

$$s_A = \sqrt{S_{a_1}^2 + S_{a_2}} = 0.22 \tag{58}$$

So we see that the distribution is not isotropic.

4.4.3 Assignment of the $\gamma - \gamma$ cascade

Next we want to find out which $\gamma - \gamma$ cascade (A $\rightarrow$ B $\rightarrow$ C) describes our data the best. Therefore we have to figure out which cascades are possible and then look which cascade fits our data the best.

- Our data obviously couldn't be fitted with $a_2 = 0$. So we need to have a $cos(\Theta)^4$ contribution, what means, that the radiation can't be a dipole radiation and has to be at least quadrupole radiation. We tried to fit with another parameter a_3 and the $cos(\Theta)^6$ contribution, but the parameter was within its error zero, so we can assume, that we just have quadrupole radiation. Since the cascade should be symmetric we have $\Delta I = 2$ for both decays, what means we have a angular moment of $l = 2$ in the radiation field of both decays.
- We know that our nucleus ($^{106}_{46}Pd$) has 46 protons and 60 neutrons, so we have a even-even nucleus and therefore we know that in its ground state it has no spin and the parity is $P = (-1)^l = 1$. So we get $I_C = 0^+$.

So after figure (5) we have three possible cascades left and we made for everyone the χ^2 test to see what cascade fits best to our parameters:

$I_A(l_1)I_B(l_2)I_C$	a_1	a_2	$\frac{\chi^2}{dof}$
0(2)2(2)0	-3	4	7.66
2(2)2(2)0	$-15/13$	16/13	152.23
4(2)2(2)0	$-1/8$	1/24	378.7

As you can see the 0(2)2(2)0 cascade fits the best to our parameters. And we have the theoretical anisotropy of

$$A = \sum_{i=1}^{2} a_i = -3 + 4 = 1 \tag{59}$$

In the following plots you can see the comparison of the theoretical angular distributions. The first one shows the pure theoretical angular distribution without convolution. The green curve is with the parameters from figure (5) and the purple with the parameters we measured. The second plot shows the datafit (Orange) and the distribution with the parameters from figure (5) but with the convolution we used to do the fit.

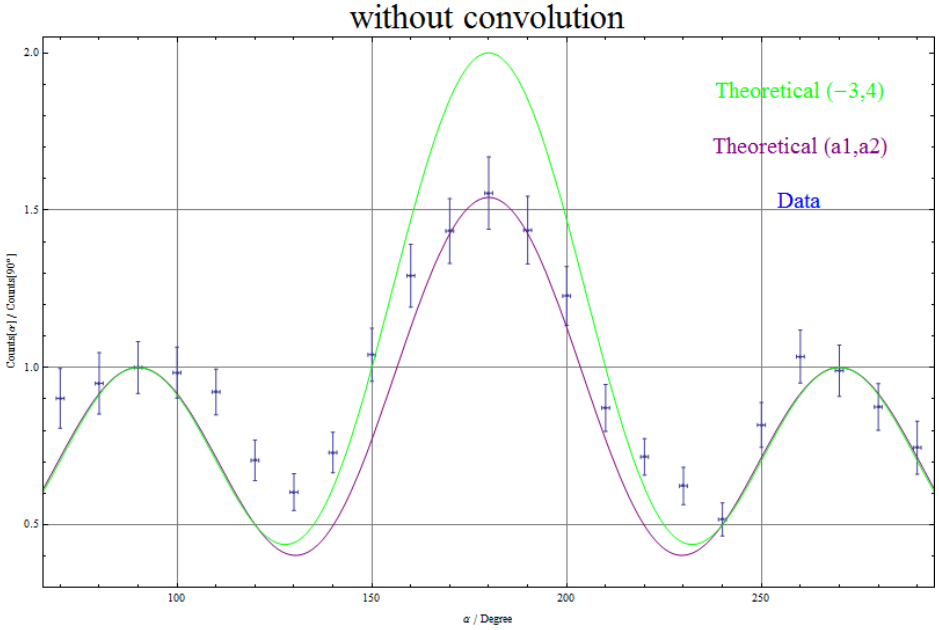

Figure 27: Comparison of the theoretical distributions and the fitted data without convolution

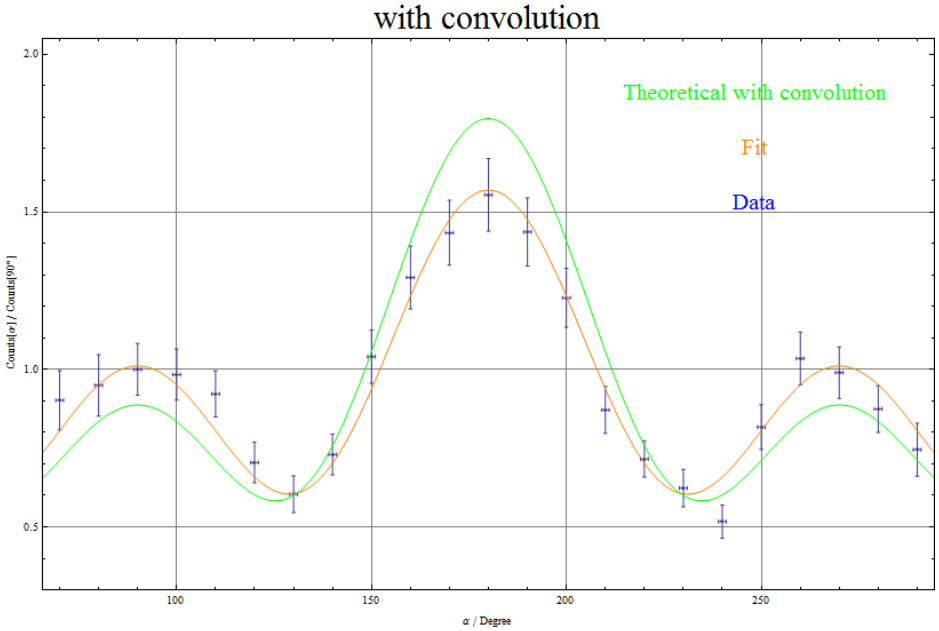

Figure 28: Comparison of the theoretical distributions and the fitted data with convolution

4.4.4 Verifying the angular resolution

As mentioned before the angular resolution measurement was a huge source for systematic errors, even if the effects where insignificant. So with the theoretical angular distribution we tried to fit the width of the Gaussian curve for the convolution to verify our angular resolution measurement.

$$\widehat{g_5}(x) = h_1 \cdot \sum_{\Theta=0}^{360} W(-3, 4, \Theta) \cdot G(x, \Theta, \sigma) \tag{60}$$

with h_1 and σ as fitting parameters.

	Estimate	Standard Error
h1	0.982039	0.0299964
s1	12.9934	1.88193

$\frac{\chi^2}{dof} = 39.86$

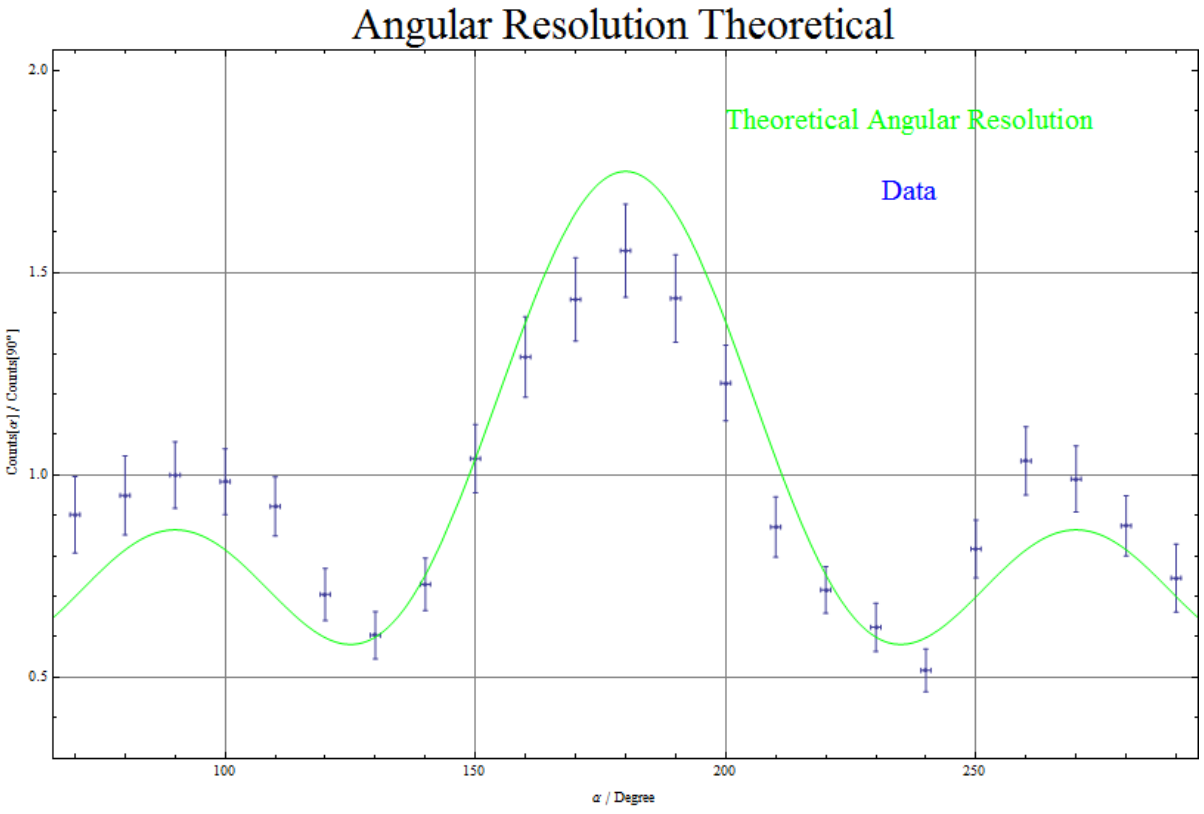

Figure 29: Theoretical Angular Resolution

As you can see the data doesn't fit perfectly. But since the width of the Gaussian curve is within its error the same we measured, we must look for another source of systematical errors.

V Conclusion

5.1 Delay

The measurement of the delay in respect to the count rate let us chose the necessary delay between the two coincident γ-emissions, which occurs because of the different way of the two photons until their measurement. We chose the adjustment of the delays d_1 and d_2 of the both SCA's, where we could see a maximum of the rate:

$$d_1 = 0.222\mu s$$
$$d_2 = 0.06\mu s$$

5.2 Energy Calibration & Palladium Spectrum

We calibrated the MCA with different probes with known energy spectres and a got for the standard curve:

$$E(Ch) = a \cdot Ch + c$$
$$a = (1.84 \pm 0.02)\text{keV}$$
$$c = -44 \pm 12$$

Where Ch is the channel number. And found three peaks in the Palladium spectrum, their energy positions we could calculate with the standard curve.

$$E_1 = (513 \pm 14)keV$$
$$E_2 = (620 \pm 15)keV$$
$$E_3 = (1097 \pm 19)keV$$

Unfortunately we couldn't fit a bigger energy range at the channels, because the calibration peaks of Sodium and Cobalt couldn't be detected any more. Therefore we couldn't find the other two peaks we wanted to detect.

5.3 Angular resolution

We measured the angular resolution three times and found out, that the probe was off-centered. To verify, that the position of the probe didn't effect the angular resolution, we placed the probe off-centered at both directions and measured again. We found out, that this shift didn't had a big effect on the measurement and we got the angular resolution a Gaussian function with the width of

$$\sigma = (12.5 \pm 0.2)^\circ \tag{61}$$

5.4 Angular correlation

5.4.1 Random coincidences

We measured a counting rate of

$$N_{Random} = (0.025 \pm 0.001)\frac{1}{s} \tag{62}$$

for the random coincidences.

5.4.2 Angular distribution

To get the parameters needed to determine the correct angular distribution, we had to fit a convolution of the theoretical angular distribution and a Gaussian function with the width we determined before from the angular resolution. Since we had systematic errors (f.e. shift) in the angular resolution measurement, we had to confirm, that these errors doesn't effect the fit parameters that much. We also showed, that the error of the angular resolution is insignificant as well.
As a result we got the angular resolution

$$W(\Theta) = (1.14 \pm 0.04) \cdot \left(1 + (-2.84 \pm 0.15) \cdot cos(\Theta)^2 + (3.38 \pm 0.16) \cdot cos(\Theta)^4\right) \tag{63}$$

and the anisotropy

$$A = (0.5 \pm 0.2) \tag{64}$$

5.4.3 Assignment of the $\gamma - \gamma$ cascade

With the parameters we could easily find out that the spin series of the $\gamma - \gamma$ cascade is $0 \rightarrow 2 \rightarrow 0$. And therefore the theoretical angular distribution should be

$$W(\Theta) = 1 - 3 \cdot cos(\Theta)^2 + 4 \cdot cos(\Theta)^4 \tag{65}$$

That means the theoretical value for the parameter a_1 is in 2-sigma-range of the measured value and for a_2 it's in the 4-sigma-range. The theoretical anisotropy is

$$A = -3 + 4 = 1 \tag{66}$$

and so it's in 3-sigma-range of the measured value.

5.4.4 Verifying the angular resolution

With the theoretical angular distribution, we tried to reconstruct the angular resolution and got the width of a Gaussian function

$$\sigma = (13 \pm 2)^\circ \tag{67}$$

You can see, it's in 1-sigma-range of the measured value. This shows again, that the main systematic error wasn't necessarily the angular resolution. We suspect the random coincidence measurement for the difference of our parameters to the theoretical prognosis.
We saw that an offset effected the fit parameters dramatically. And since we did measure over night it's very likely that there were the same effects as in our third measurement. We may also should have measured the random coincidences for every angle to be sure, that they are uniformly distributed.

Bibliography

[1] Instructions:
http://wwwhep.physik.uni-freiburg.de/fp/Versuche/FP2/FP2-6-Winkelkorrelation/Anleitung.pdf

[2] Angular Correlation of Successive Radiations:
http://wwwhep.physik.uni-freiburg.de/fp/Versuche/FP2/FP2-6-Winkelkorrelation/Anhang/Weiter-Literatur/S-49-56-Angular-Corr.-Successive%20Rad..pdf

[3] Demtroeder Experimentalphysik 4 (3.edition)

[4] Mayer-Kuckuk Kernphysik (6.edition)

[5] Report on Progress in Physics by Martin Deutsch 1951:
http://wwwhep.physik.uni-freiburg.de/fp/Versuche/FP2/FP2-6-Winkelkorrelation/Anhang/Weiter-Literatur/S-57-64-M.Deutsch.pdf

[6] Dipolstrahlung by F.Fischer: http://wwwhep.physik.uni-freiburg.de/fp/Versuche/FP2/FP2-6-Winkelkorrelation/Anhang/Weiter-Literatur/S-27-48a-F.Fischer.pdf

[7] Staatsexamen of Tpboijas Kotyk:
http://james.physik.uni-freiburg.de/fp/Versuche/FP1/FP1-7-LangeHalbwertzeiten/Staatsex-Lange-Hwz.pdf

[8] P. Marnier:
http://wwwhep.physik.uni-freiburg.de/fp/Versuche/FP2/FP2-6-Winkelkorrelation/Anhang/Weiter-Literatur/S-1-18-P.Marnier.pdf

VI Appendum

6.1 Manually noted data

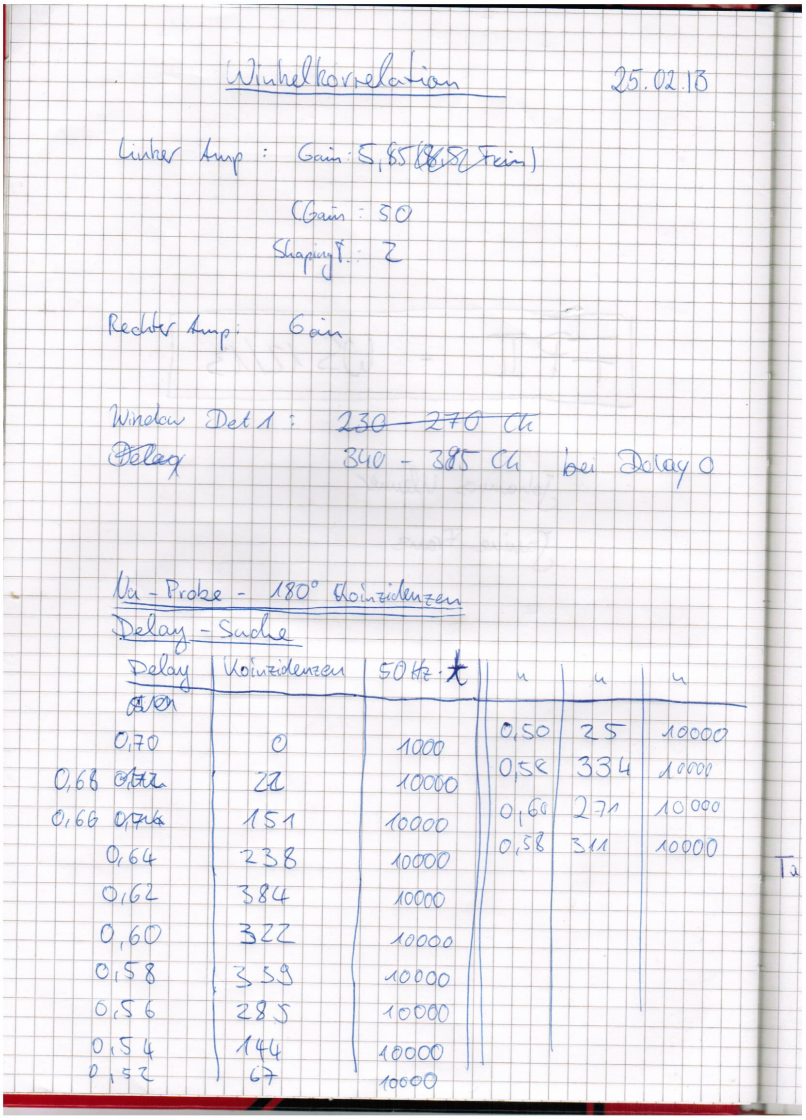

Winkelkorrelation 25.02.13

Linker Amp: Gain 5,85 (Fein)

Gain: 50

Shaping t.: 2

Rechter Amp: Gain

Window Det 1: ~~230 - 270 Ch~~

Delay 340 - 385 Ch bei Delay 0

Na-Probe - 180° Koinzidenzen

Delay-Suche

Delay	Koinzidenzen	50 Hz · t			
~~0,70~~					
0,70	0	1000	0,50	25	10000
~~0,68~~	~~22~~	10000	0,58	33,4	10000
~~0,66~~	151	10000	0,60	27,1	10000
0,64	238	10000	0,58	31,1	10000
0,62	384	10000			
0,60	322	10000			
0,58	359	10000			
0,56	285	10000			
0,54	144	10000			
0,52	67	10000			

Figure 30: Page 1/12

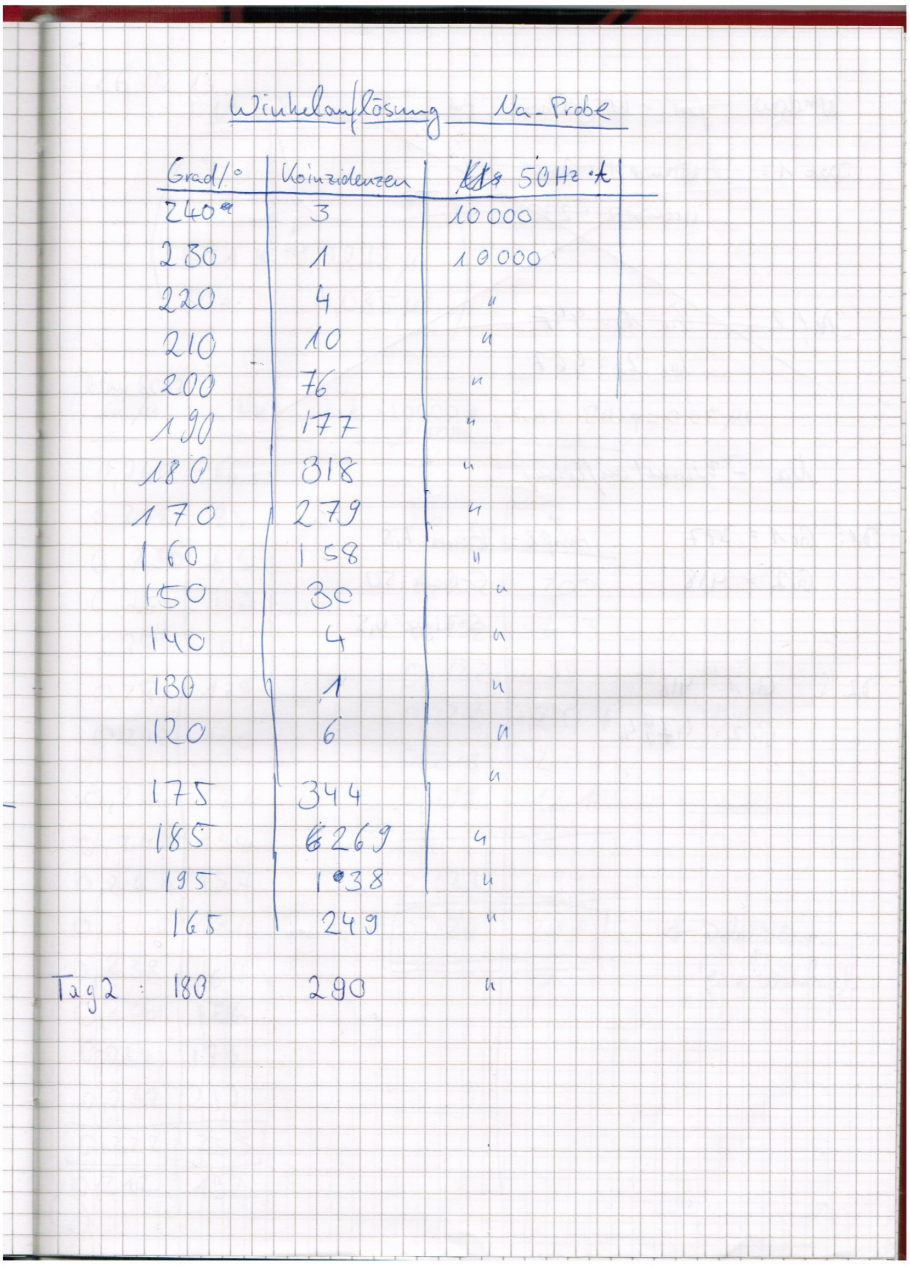

Winkelauflösung Na-Probe

Grad/°	Koinzidenzen	50 Hz · t
240°	3	10000
230	1	10000
220	4	"
210	10	"
200	76	"
190	177	"
180	318	"
170	279	"
160	158	"
150	30	"
140	4	"
130	1	"
120	6	"
175	344	"
185	6269	"
195	1038	"
165	249	"
Tag 2: 180	290	"

Figure 31: Page 2/12

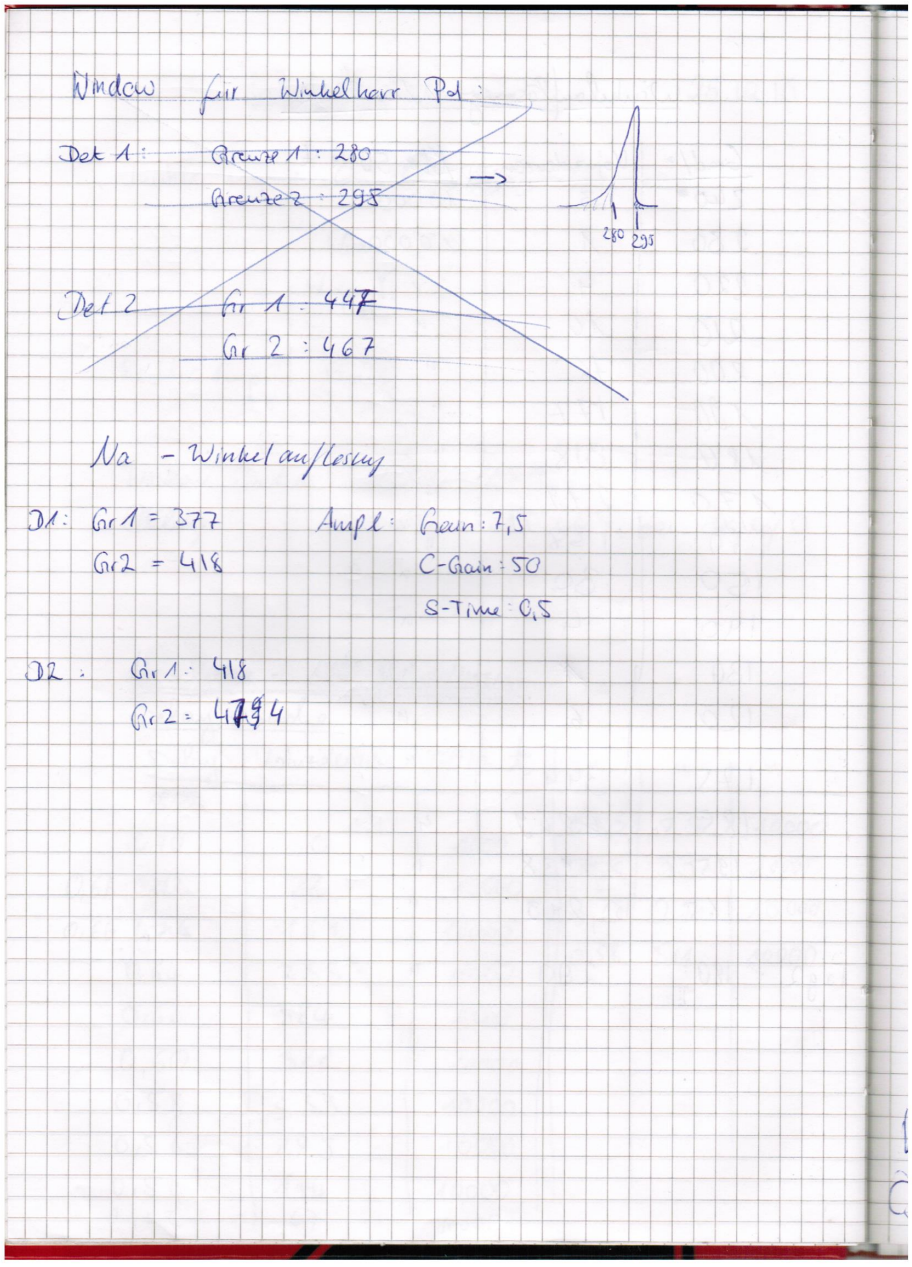

Figure 32: Page 3/12

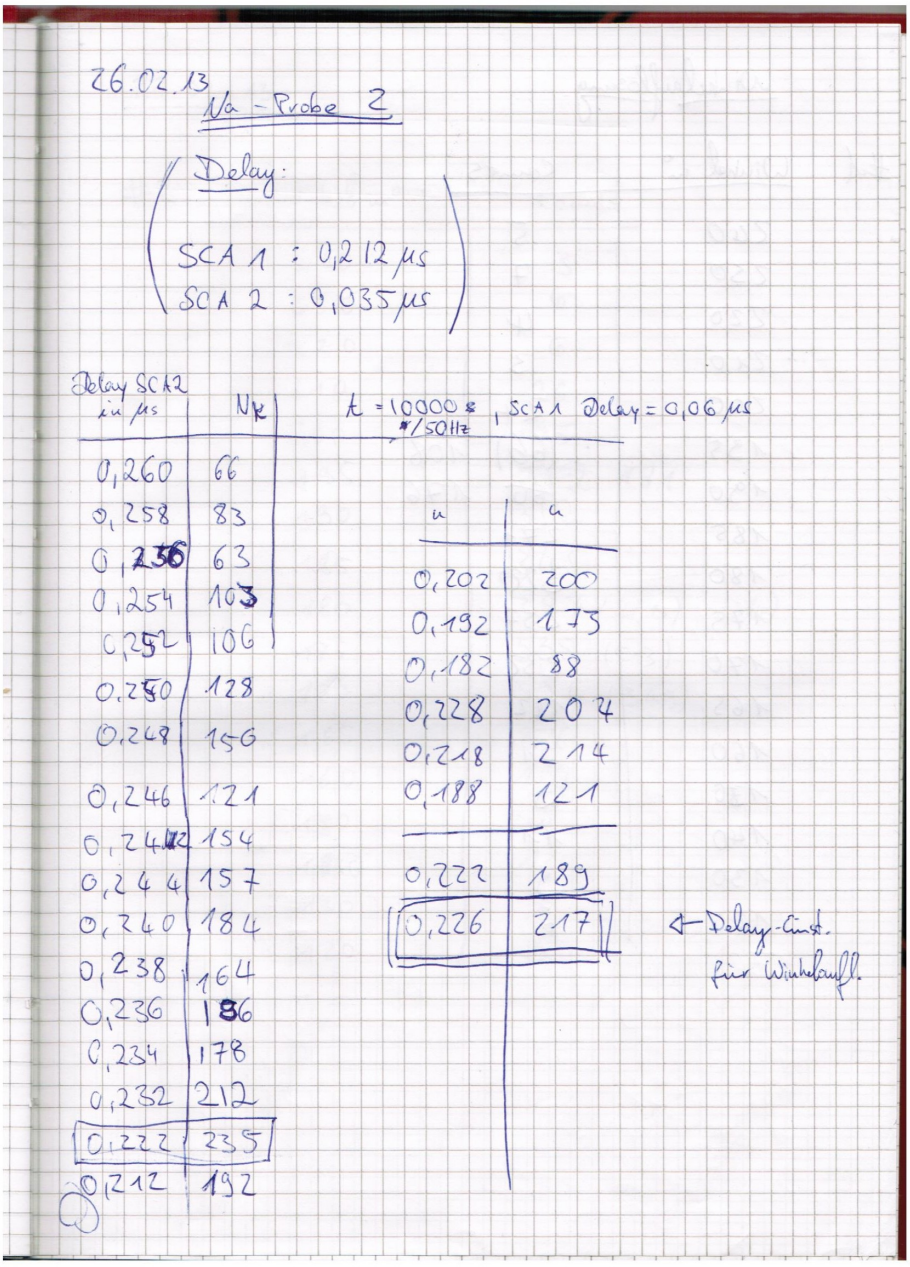

Figure 33: Page 4/12

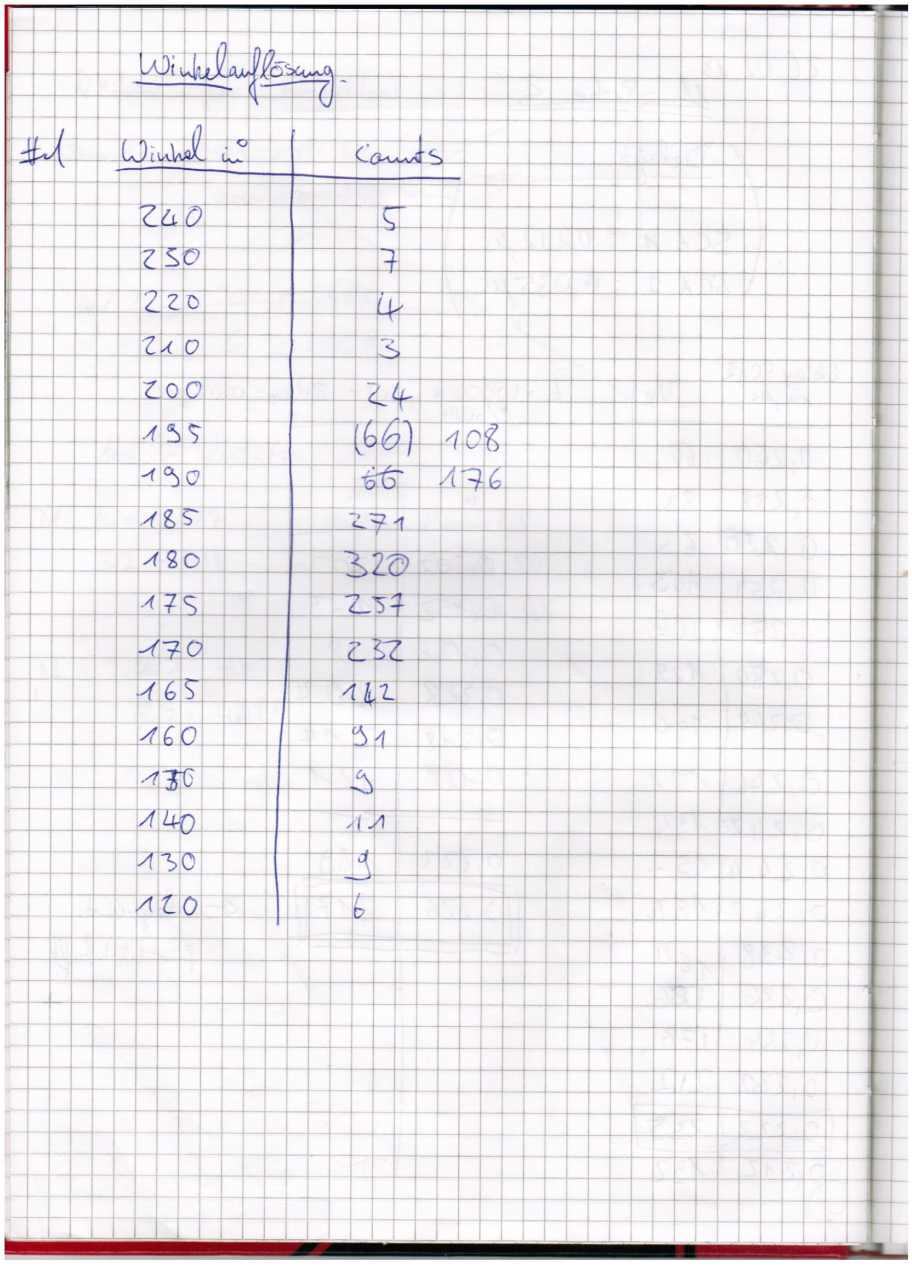

Winkelauflösung

#d	Winkel in °	counts	
	240	5	
	230	7	
	220	4	
	210	3	
	200	24	
	195	(66)	108
	190	~~66~~	176
	185	271	
	180	320	
	175	257	
	170	232	
	165	142	
	160	91	
	~~150~~	9	
	140	11	
	130	9	
	120	6	

Figure 34: Page 5/12

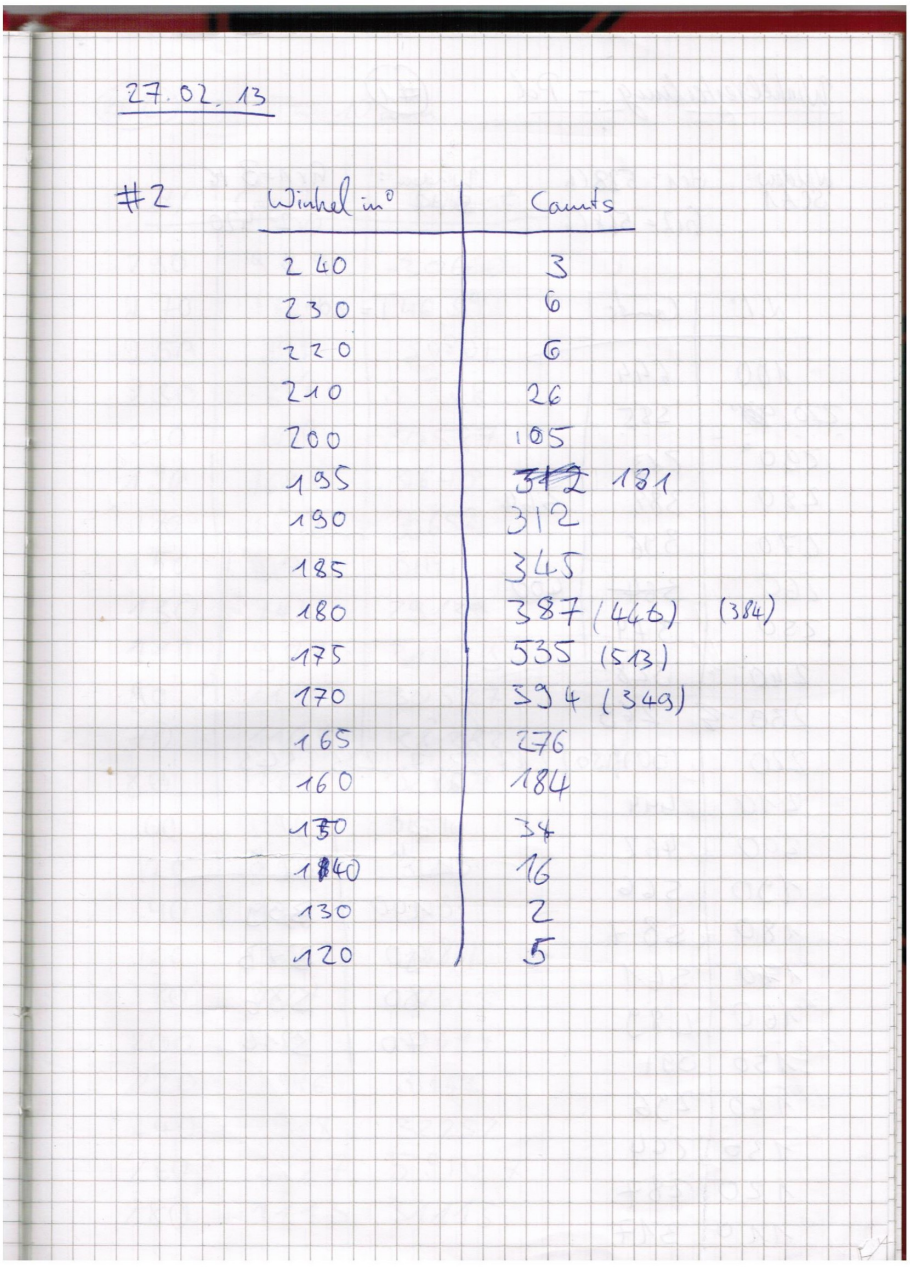

27.02.13

#2

Winkel in°	Counts
240	3
230	6
220	6
210	26
200	105
195	~~312~~ 181
190	312
185	345
180	387 (466) (384)
175	535 (513)
170	394 (349)
165	276
160	184
~~150~~	34
~~140~~	16
130	2
120	5

Figure 35: Page 6/12

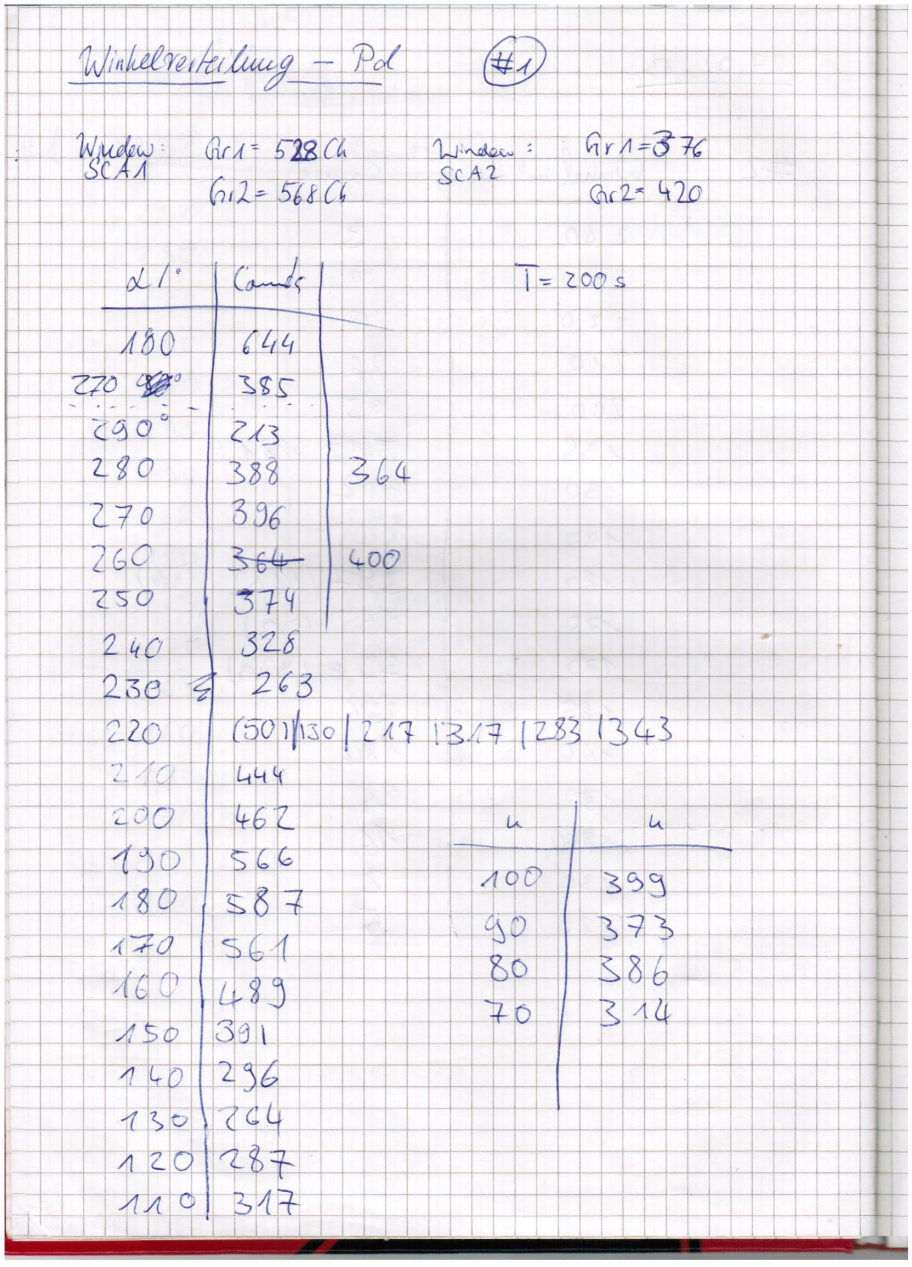

Winkelverteilung – Pol (#1)

Window: SCA1 Gr1 = 528 Ch Gr2 = 568 Ch

Window: SCA2 Gr1 = 376 Gr2 = 420

T = 200 s

α / °	Counts	
180	644	
270 ~~280~~	385	
~~290~~	213	
280	388	364
270	396	
260	~~364~~	400
250	374	
240	328	
230	263	
220	(501)130 | 217 | 317 | 283 | 343	
210	444	
200	462	
190	566	
180	587	
170	561	
160	489	
150	391	
140	296	
130	264	
120	287	
110	317	

u	u
100	399
90	373
80	386
70	314

Figure 36: Page 7/12

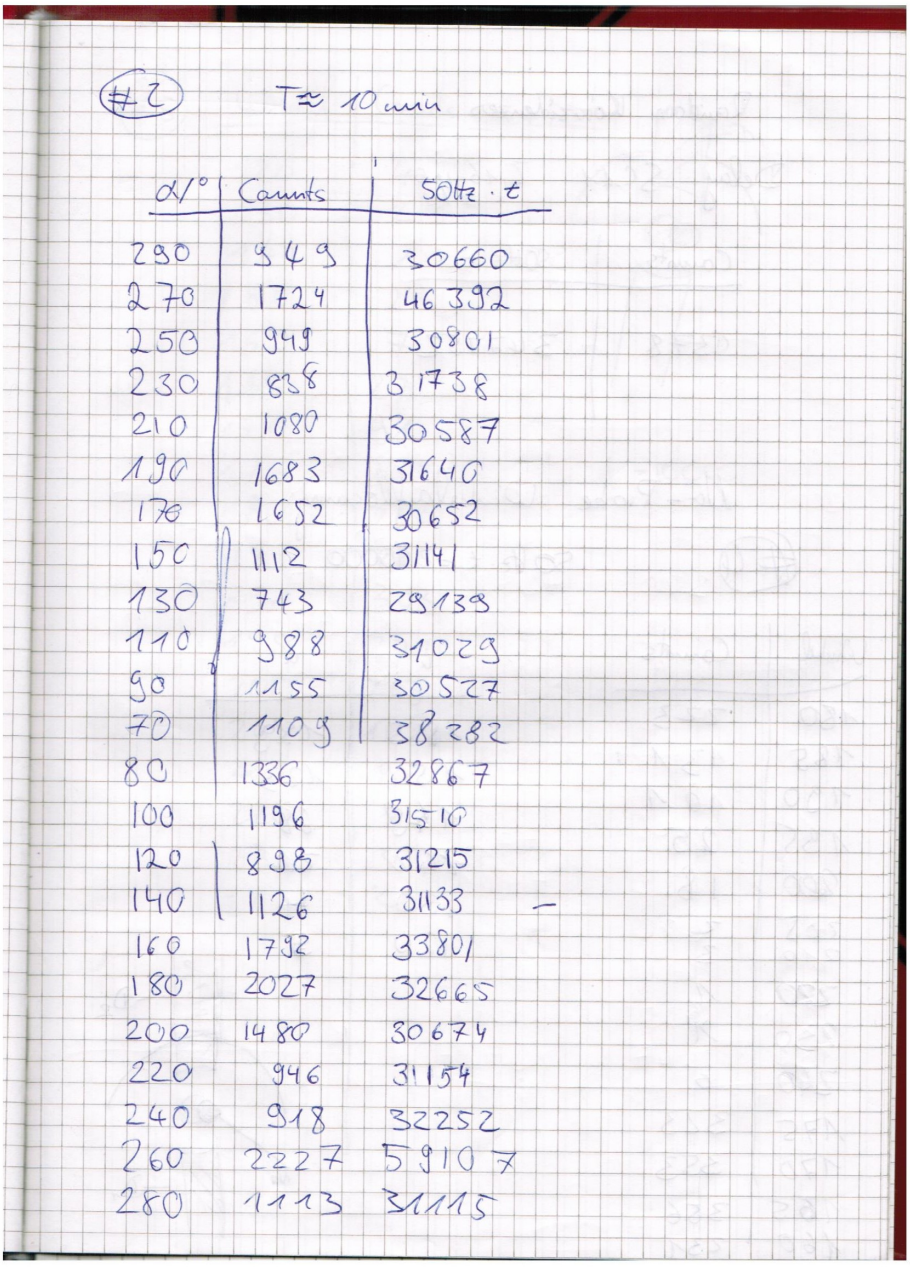

#2 T≈ 10 min

α/°	Counts	50Hz · t
290	949	30660
270	1724	46392
250	949	30801
230	858	31738
210	1080	30587
190	1683	31640
170	1652	30652
150	1112	31141
130	743	29139
110	988	31029
90	1155	30527
70	1109	38282
80	1336	32867
100	1196	31510
120	898	31215
140	1126	31133
160	1792	33801
180	2027	32665
200	1480	30674
220	946	31154
240	918	32252
260	2227	59107
280	1113	31115

Figure 37: Page 8/12

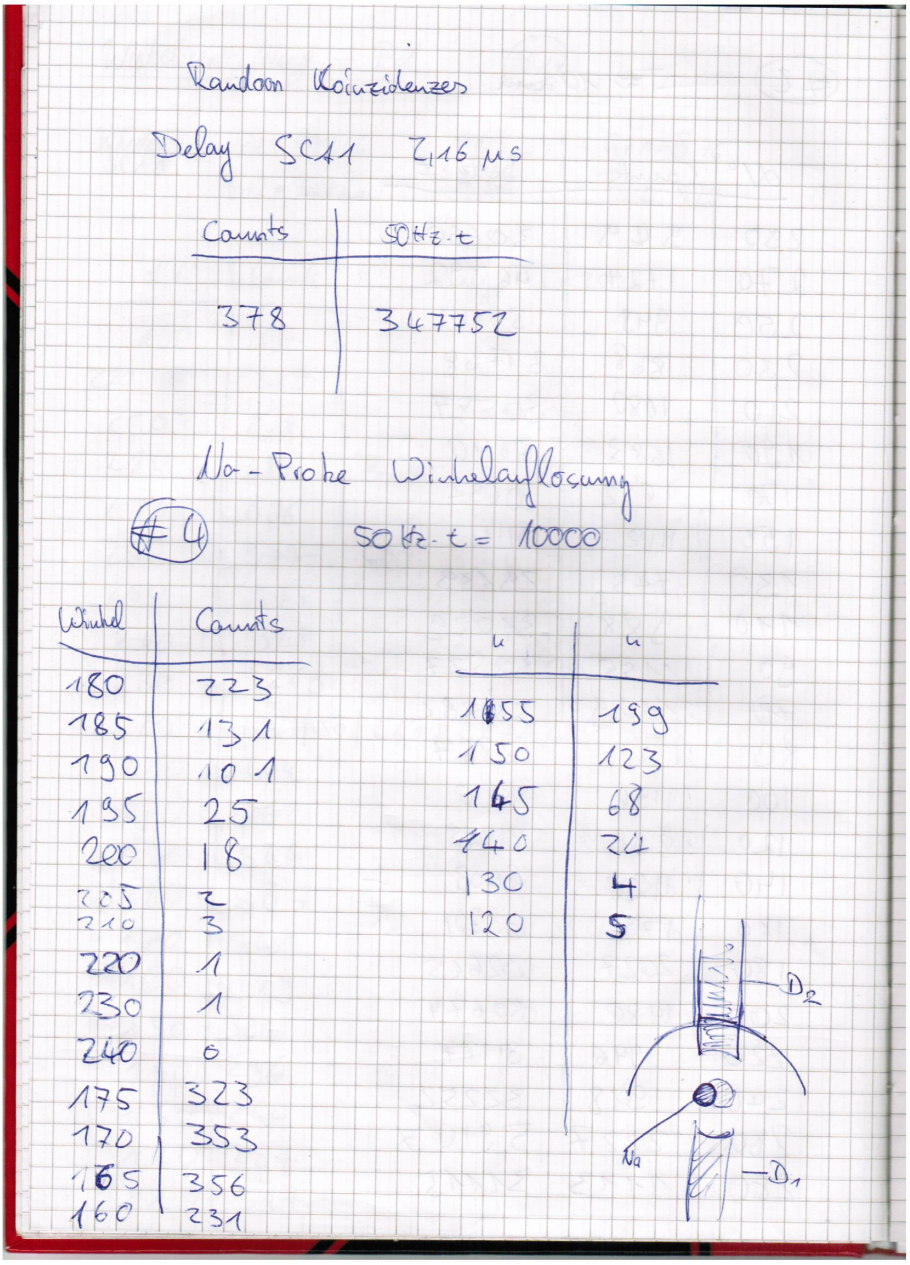

Figure 38: Page 9/12

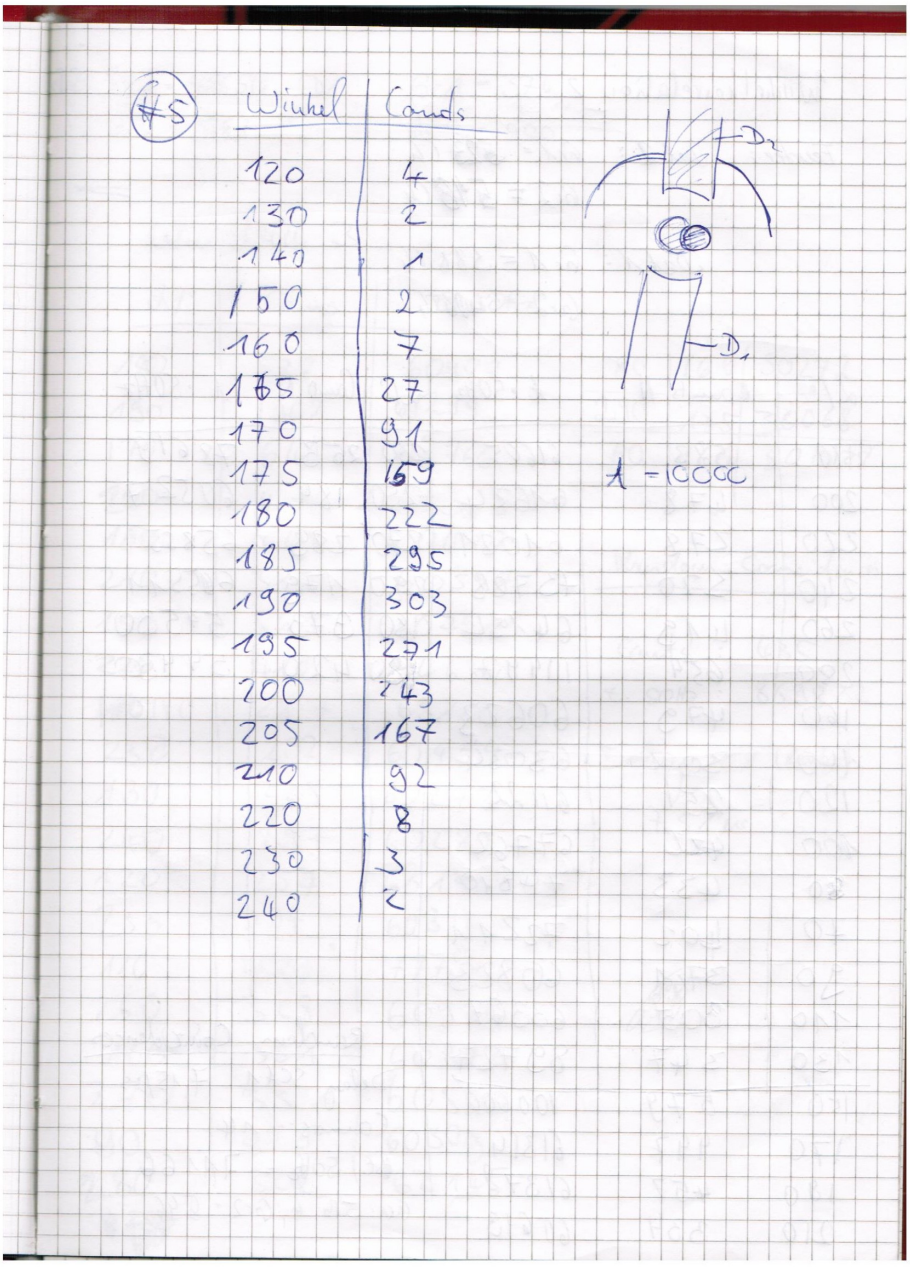

Figure 39: Page 10/12

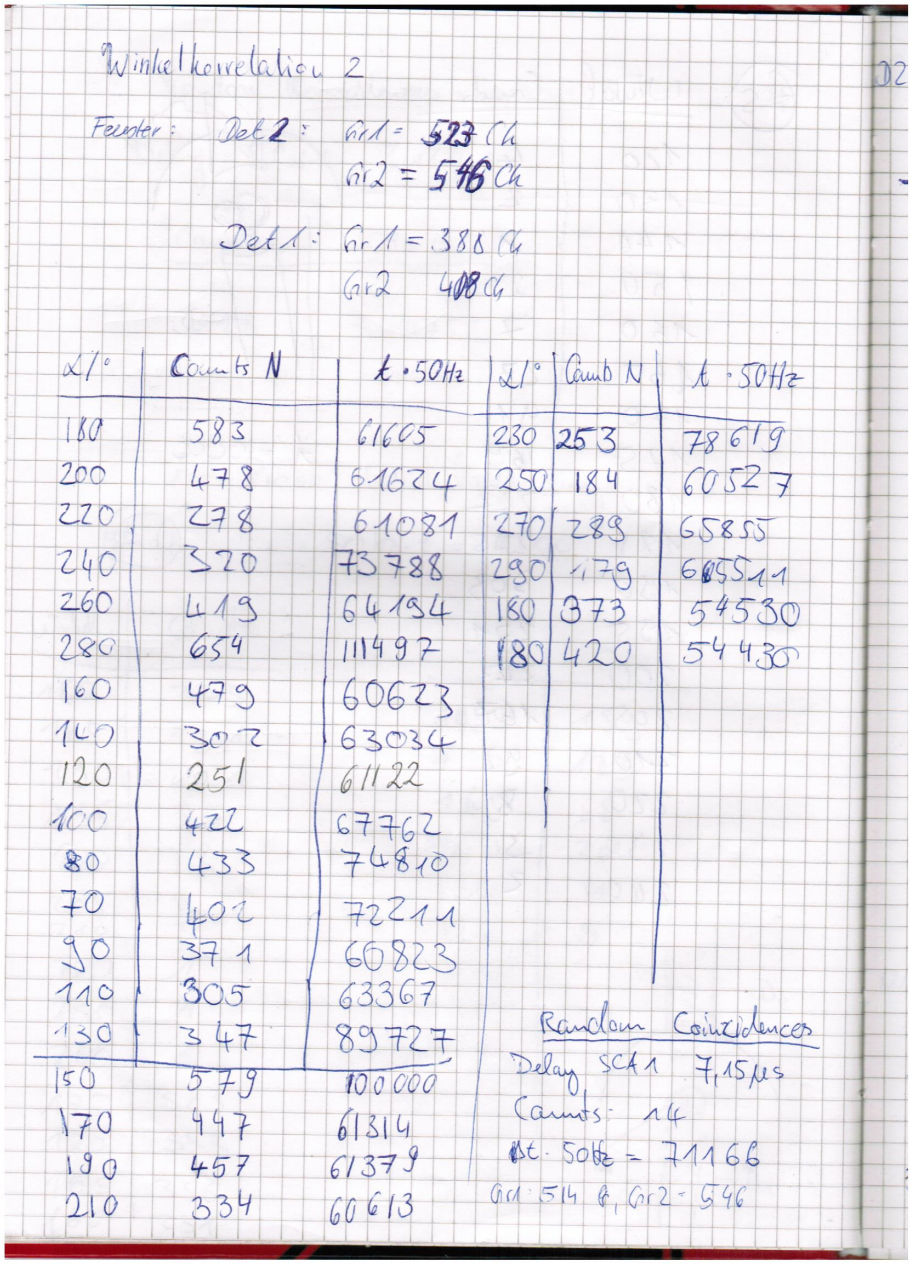

Winkelkorrelation 2

Fenster: Det 2: Gr 1 = 523 Ch
Gr 2 = 546 Ch

Det 1: Gr 1 = 388 Ch
Gr 2 408 Ch

α/°	Counts N	t · 50Hz
180	583	61605
200	478	61624
220	278	61081
240	320	73788
260	419	64194
280	654	111497
160	479	60623
140	307	63034
120	251	61122
100	422	67762
80	433	74810
70	402	72211
90	371	60823
110	305	63367
130	347	89727
150	579	100000
170	447	61314
190	457	61379
210	334	60613

α/°	Counts N	t · 50Hz
230	253	78619
250	184	60527
270	289	65855
290	179	68511
180	373	54530
180	420	54430

Random Coincidences
Delay SCA 1 7,15 µs
Counts: 14
Akt. Sollz = 71166
Gr1 514 6, Gr2 546

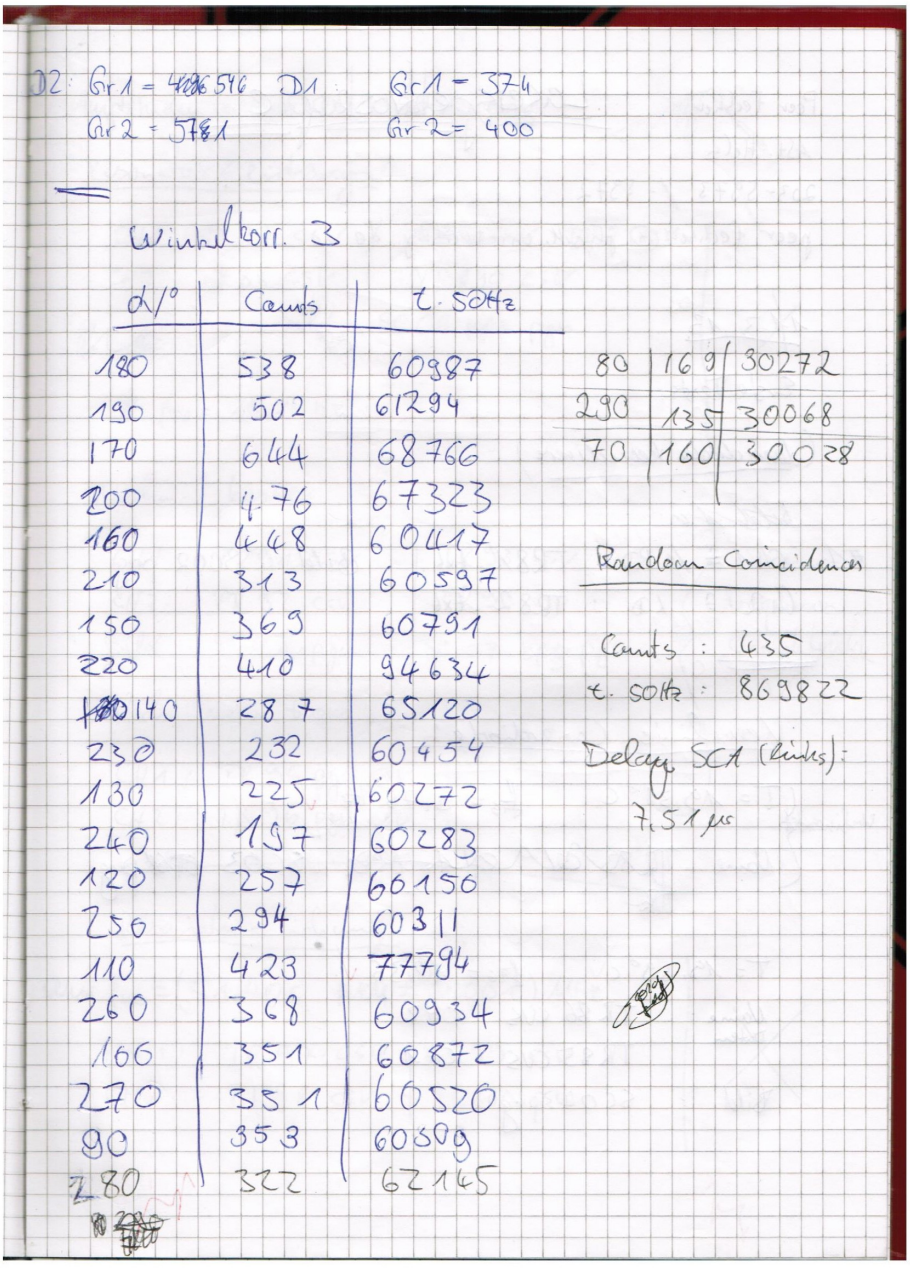

D2: Gr 1 = 546 D1: Gr 1 = 374
Gr 2 = 5781 Gr 2 = 400

Winkelkorr. 3

α/°	Counts	t. 50Hz
180	538	60987
190	502	61294
170	644	68766
200	476	67323
160	448	60417
210	313	60597
150	369	60791
220	410	94634
140	287	65120
230	232	60454
130	225	60272
240	197	60283
120	257	60156
250	294	60311
110	423	77794
260	368	60934
100	351	60872
270	351	60520
90	353	60509
280	322	62165

80	169	30272
290	135	30068
70	160	30028

Random Coincidences

Counts : 435
t. 50Hz : 869822

Delay SCA (links):
7,51 µs